ASTRONOMY & ASTROPHYSICS
SUPPLEMENT SERIES

Astron. Astrophys. Suppl. Ser. **139**, 277–295 (1999)

A ROSAT PSPC catalogue of X-ray sources in the LMC region

F. Haberl and W. Pietsch

Max–Planck–Institut für extraterrestrische Physik, Giessenbachstraße, 85748 Garching, Germany

Received April 30; accepted July 9, 1999

Abstract. We analyzed more than 200 ROSAT PSPC observations in a 10 by 10 degree field centered on the Large Magellanic Cloud (LMC) and performed between 1990 and 1994 to derive a catalogue of X-ray sources. The list contains 758 sources with their X-ray properties. From cross-correlations of the PSPC catalogue with the SIMBAD data base and literature searches we give likely identifications for 144 X-ray sources based on positional coincidence, but taking into account X-ray properties like hardness ratios and source extent. 46 known sources are associated with supernova remnants (SNRs) and candidates in the LMC, most of them already detected by previous X-ray missions. Including the new candidates from Haberl & Pietsch (1999) based on variability studies of the sources in our PSPC catalogue, the number of X-ray binaries in the LMC increased to 17 and that of the supersoft sources (SSSs) to 9. The remaining ∼50% of the identified sources comprise mainly foreground stars (up to 57) and background extragalactic objects (up to 15). The often distinguished X-ray properties of the different source types were used for a first classification of new, unknown X-ray sources. Eight new PSPC sources are classified as SNRs from their hardness ratios and one promising new SNR candidate with extended X-ray emission is found further north than all known SNRs. Three soft X-ray sources have hardness ratios compatible to those of the known SSSs. A selection on hardness ratios and X-ray to optical flux ratio further suggests 27 foreground stars and 3 AGN.

Key words: catalogues — galaxies: magellanic clouds — galaxies: stellar content — X-rays: galaxies — X-rays: stars

1. Introduction

The first soft X-ray survey of the LMC with imaging instruments was performed with the Einstein satellite (Long et al. 1981, hereafter LHG81; Wang et al. 1991, hereafter WHHW91). More than 100 discrete X-ray sources were detected and in addition large-scale diffuse emission originating from hot gas with temperatures of several 10^6 K was revealed. About 50% of the point-like sources were identified with objects in the LMC, while the remainder was assigned to galactic foreground stars and background AGN. Due to the vicinity to the south ecliptic pole the LMC was observed with high sensitivity by the Position Sensitive Proportional Counter (PSPC) during the ROSAT all-sky survey (RASS). For a description of the ROSAT mission and PSPC detector see Trümper (1983) and Pfeffermann et al. (1986). Pietsch & Kahabka (1993) analyzed a $13^\circ \times 13^\circ$ area centered on the LMC and found more than 500 X-ray sources.

Large-scale radio surveys of the LMC were performed using the Parkes 64 m radio telescope at different frequencies (Filipović et al. 1995). A comparison of the radio source catalogue with the ROSAT survey catalogue of Pietsch & Kahabka (1993) yielded 71 sources within a correlation radius of $2.5'$ (Filipović et al. 1996). These are mainly SNRs and extragalactic objects.

Pointed ROSAT PSPC observations from independent scientific programs covered large parts of the LMC and first mosaic images have been published by Snowden & Petre (1994). Here we present the first results of a systematic study of the PSPC observations to derive a catalogue of point(-like) sources in the LMC. Cross-correlations with catalogues from other wavelength bands yield first identifications and allow to derive classification schemes for the new, unidentified sources. Based on this one can pre-select candidate samples for various source classes like SNRs, X-ray binaries and SSSs in the LMC and to distinguish them from foreground stars and background AGN.

2. ROSAT PSPC observations and analysis

During the nominal operation phase of the PSPC between 1990 and 1994 this imaging X-ray detector on board ROSAT was used for more than 200 pointed

Send offprint requests to: F. Haberl (fwh@mpe.mpg.de)

observations in an area of $10^\circ \times 10^\circ$ centered on the position RA = 05^h 25^m 00^s Dec = -67° $43'$ $20''$. The often overlapping images cover in total 58.6 square degrees of the LMC region. A merged image in the energy band 0.5 − 0.9 keV with a resolution of $15''$ is presented in Haberl & Pietsch (1998). Statistics about the location and exposures of the PSPC observations can be found in Haberl & Pietsch (1999), hereafter HP99. For our analysis we used the 212 observations with exposure of more than 100 s.

Using merged data for source detection is only useful in areas where data from the central part of the detector is not superposed by off-axis data with degraded spatial resolution. To derive a catalogue of point and point-like X-ray sources in the LMC we therefore started with the analysis of the images from the individual observations. Each of the 212 observations has been analyzed in five energy bands (soft: 0.1−0.4 keV, hard: 0.5−2.0 keV, hard1: 0.5−0.9 keV, hard2: 0.9 − 2.0 keV and broad 0.1 − 2.4 keV) with the three detection methods of EXSAS (Zimmermann et al. 1994). For each band the merged detection lists of two sliding box methods (using local background and a spline fit background map) were used as input for the maximum likelihood (ML) algorithm. Sources were only accepted when the likelihood of existence (ML_{exi}) was larger than 10.0 (corresponding to a probability $P = 1 - \exp(-ML_{exi})$ greater than $1 - 4.5\ 10^{-5}$), the total number of counts more than 12 and the angle to the telescope axis within $52'$. The five ML detection lists from the different bands were merged to a single list for each observation. The ML results were used for the final source parameters like likelihood of existence, celestial coordinates, detected counts, source extent and extent likelihood. For all parameters uncertainties are given.

The source extent was determined using a Gaussian approximation for the intensity profile. This is justified as long as the extent is small and the surface brightness distribution is well peaked in the center. However there are well known SNRs in the LMC which do not obey these criteria (in particular ring shaped remnants like N 132D). The maximum likelihood algorithm gives too low count rates in these cases. This effect is strongest in the center of the field of view (FOV) of the instrument and decreases with off-axis angle due to the degrading point spread function (PSF) which smears out any structures. As a consequence we re-determined the number of detected source counts by integrating them in a box around the source and a nearby box for background for the following SNRs: N 132D, N 63A, N 49, N 103B and N 49B.

To determine count rates, exposure maps were created taking instrument maps (vignetting) and the satellite attitude into account. From the count rates in the soft (S), hard (H), hard1 (H1) and hard2 (H2) bands hardness ratios HR1 = (H − S)/(S + H) and HR2 = (H2 − H1)/(H1 + H2) were derived as indicators for the shape of the X-ray spectrum. A mask of the support structure of the detector entrance window and the detector rim (WSS) was summed up taking the changing attitude (mainly caused by the satellite wobble) into account. This "wobbled mask" was used to calculate the distance of each source to the shadowed structures where the exposure was reduced by more than 10%. The distance in units of the $FWHM$ of the point spread function directly gives an indication for how much source parameters are influenced by the WSS.

A large fraction of the LMC region was observed more than once yielding multiple detections of many sources. To study long-term time variability HP99 cross-correlated the detection lists of all individual observations. They presented 27 X-ray sources which showed flux variations as observed by the PSPC by factors between 3 and more than 1000.

For this work the detection lists were merged to produce a source catalogue of ROSAT PSPC sources. For sources with multiple detections the one with the smallest position error (usually the detection nearest to the telescope axis and/or best counting statistics) entered the catalogue. Two detections were regarded as caused by the same source when their positions are within the distance $d = d_{90} + d_{\rm ext}$, where d_{90} denotes the summed 90% errors of the two sources and the systematic error of $7''$ and $d_{\rm ext}$ the average source extent of the two detections. The source extent was only used when the likelihood for the extent was larger than 20. The catalogue was finally visually screened to remove spurious detections like multiple detections in diffuse emission regions and obvious false detections near the WSS. In particular in the 30 Doradus region the intense diffuse X-ray emission led to many spurious detections which were screened out. Only known SNRs were accepted and for a more complete catalogue in that area HRI data with better angular resolution needs to be analyzed. The final PSPC catalogue of point-like and weakly extended sources comprises 758 entries. An excerpt with five consecutive entries is shown in Table 1. The complete table is available electronically. The table columns give (1) source number, (2) likelihood of existence (maximum value from the five detection energy bands), (3) net exposure, vignetting corrected, (4) and (5) celestial coordinates of X-ray source, derived from energy band with lowest position error, (6) statistical 90% confidence error on the X-ray position, the systematic uncertainty is about $7''$, (7) PSPC 0.1−2.4 keV count rate and error, (8) and (9) hardness ratios, not calculated in cases where not all required count rates are available, (10) source extent, from same detection as source position, (11) likelihood for the extent, (12) ROSAT observation identifier, (13) off-axis angle, (14) distance to WSS and (15) remark.

Table 1. Excerpt of the catalogue of 758 PSPC sources from a $10° \times 10°$ field centered on the LMC

1	2	3	4	5	6	7	8	9	10	11
No	ML_{exi}	Exp. [s]	RA (J2000.0)	Dec	r_{90} [″]	Count Rate [cts s^{-1}]	HR1	HR2	Extent [″]	ML_{ext}
183	357.9	43636	05 30 10.6	−65 51 27	2.8	6.00e-03 ± 4.5e-04	1.00 ± 0.21	0.62 ± 0.07	1.6	0.0
184	531.3	40488	05 32 32.0	−65 51 42	3.3	1.11e-02 ± 6.3e-04	1.00 ± 0.10	0.43 ± 0.05	10.7	15.4
185	12.0	39771	05 32 14.0	−65 52 09	12.6	7.50e-04 ± 7.5e-04	1.00 ± 0.51		0.0	0.0
186	36.3	5318	05 27 23.7	−65 52 35	15.9	9.57e-03 ± 1.7e-03	1.00 ± 0.36	0.29 ± 0.19	24.2	16.0
188	23.9	5937	05 20 16.7	−65 53 15	29.7	6.14e-03 ± 1.5e-03			13.2	0.1

12	13	14	15
ROR	δ [′]	d_{rib} [$FWHM$]	Remark
200692p	5	21.3	[hard]
200692p	12	10.5	HMXB OB variable RXJ0532.5 − 6551, Sk −65 66 (HPD95 HP99)
200692p	10	13.7	
500062p	14	6.4	
500053p	25	0.2	

3. Comparison with existing catalogues

3.1. Correlation with the Einstein survey

The first comprehensive X-ray survey of the LMC was performed with the Einstein Observatory in the energy range $0.15 - 4$ keV. Catalogues of discrete sources derived from the Imaging Proportional Counter (IPC) data were published by LHG81 and after a re-analysis by WHHW91. Both lists comprise together 140 distinct X-ray sources from which 12 were not covered by PSPC pointings (within 52′). From the remaining 128 sources 78 (a fraction of 61%) were detected in the PSPC observations (within a correlation radius of 90″). In Table 2 the 50 IPC sources with no detection in the PSPC are summarized. The table gives the source number from LHG81 (Col. 1), the WHHW91 name (Col. 2), the number of PSPC observations which covered the IPC position (within 52′, Col. 3), the minimum and maximum off-axis angle (Cols. 4 and 5) and the minimum and maximum exposure (Cols. 6 and 7). 67 IPC sources in the PSPC FOV were both detected by LHG81 and WHHW91 from which 55 (82%) were detected by the PSPC. The lower PSPC detection rates of 38% (15 out of 39) IPC sources found by WHHW91 only and 36% (8/22) IPC sources found by LHG81 only are compatible with the expected higher percentage of spurious detections in these subsamples. Extrapolating from the more secure sources (those detected by LHG81 *and* WHHW91) that ∼18% of the IPC sources were not recovered by the PSPC, most likely due to time variability, results in about 50% spurious detections in the number of Einstein sources which are either only detected by LHG81 or only by WHHW91. A similar conclusion was drawn by Schmidtke et al. 1998, from ROSAT HRI observations of Einstein sources. Sources 29, 55, 58, 63, 64 and 96 from LHG81 were not detected by the HRI although the observations were sensitive enough. Neither of these sources were detected by the PSPC (96 was not in the FOV), casting doubt on their reality. Table 2 shows several additional IPC detections (e.g. sources LHG 37, 65, 75, 76, 81, 84 and WHHW 521.5 − 6921, 523.7 − 6923, 524.2 − 6937...) which were observed many times by the PSPC and never detected.

In Table 4 77 Einstein IPC sources detected by the PSPC are given. In addition to the columns described for Table 1 Col. 2 gives the source number from LHG81, Col. 3 the source name from WHHW91, Col. 4 the distance between Einstein IPC and ROSAT PSPC position and Col. 7 the IPC count rate. For source 603 the IPC sources 522.5 − 6759 and 522.6 − 6801 (WHHW91) are within the correlation radius of 90″, both are part of the HII complex N 44. To estimate the confidence of the identification, the 90% statistical error of the PSPC position is given. A systematic error of 7″ should be added. The error on the IPC position is estimated to 40″ by LHG81 (1σ).

The IPC and PSPC count rates of 76 sources from Table 4 (LMC X − 3 is not included because no IPC count rate is given in LHG81 and WHHW91) are compared in Fig. 1 where the sources identified with an SNR (see Sect. 3.3.1) are marked with a circle. A linear fit to the SNR count rates gives a mean conversion factor of 3.2 for IPC to PSPC count rates. The scatter shows however that the conversion rate is strongly dependent on the detailed X-ray spectrum and in particular on the absorption. Clear variability on long-term time scales is only seen for at most three sources: AB Dor, CAL 83 and LMC X − 4 which are known to be highly variable. The different energy bands and comparison of only two epochs makes it difficult to look for time variable sources.

Table 2. Einstein IPC sources not detected by the PSPC

1	2	3	4	5	6	7
LHG	WHHW	$N_{\rm obs}$	$\delta_{\rm min}$ [′]	$\delta_{\rm max}$ [′]	$\exp_{\rm min}$ [s]	$\exp_{\rm max}$ [s]
21	517.9-7047	4	22	51	184	443
24	519.7-7107	3	31	50	184	443
	520.8-6738	6	22	41	3420	8720
	521.5-6921	52	9	51	117	14581
	522.2-6758	5	0	46	117	8720
	523.7-6923	51	7	51	117	14581
	524.2-6937	54	4	52	141	14581
	527.6-6729	17	10	51	357	8720
	528.5-6942	66	4	51	143	16957
41	528.6-6746	9	20	50	357	8720
44	530.8-6657	30	4	51	285	14507
	534.3-7052	8	14	44	157	11303
56	535.3-6948	56	8	52	143	16957
	536.2-6912	35	6	52	143	16957
	537.0-6942	45	4	52	143	16957
	538.0-6904	28	3	47	143	16957
	538.0-6932	35	8	51	143	16957
68	538.4-6907	30	3	51	143	16957
	538.9-6914	33	6	51	143	16957
72	539.1-6908	29	1	52	143	16957
73	539.2-6911	31	4	50	143	16957
74	539.2-6904	28	5	52	143	16957
	539.4-6860	24	9	47	182	16957
	539.7-6858	24	11	48	182	16957
	539.8-6907	26	5	49	182	16957
	540.3-6909	28	8	52	182	16957
77	540.5-6927	33	6	52	143	16957
	541.0-6859	22	9	47	192	16957
	541.0-7013	21	15	47	200	11303
80	541.8-6906	26	4	51	192	16957
	543.1-6927	30	11	50	192	16957
	543.9-6934	30	9	50	192	16957
	545.9-6731	4	45	52	535	1578
	546.4-6945	18	7	47	822	8823
	553.0-6953	4	27	51	822	4021
94	553.2-6927	2	27	34	2061	4021
29		2	21	21	11277	12794
37		57	10	52	117	16957
55		45	5	51	143	16957
58		43	12	51	143	16957
63		37	7	51	143	16957
64		34	14	52	157	11303
65		28	1	48	143	16957
75		15	39	51	285	14507
76		41	4	52	143	16957
81		20	13	52	200	11303
84		18	14	47	200	8823
85		1	36	36	4566	4566
90		1	24	24	4566	4566
95		3	24	50	6039	19651

3.2. Comparison with the ROSAT all-sky survey

The Bright Source Catalogue (BSC) of the RASS was published by Voges et al. (1996). A correlation of the PSPC catalogue from the pointed observations with the BSC catalogue yields 55 sources within a distance of 60″. They are summarized in Table 5. The count rates are shown in Fig. 2. The SNR count rates scatter little around the line of ratio 1.0, as expected for constant sources. The only exception is N 49 with a too low BSC count rate. Sources variable by more than a factor of 3.0 are the high mass X-ray binary (HMXB) LMC X − 4 and the Be X-ray transient A0538 − 66 which was in outburst during the RASS (see also HP99).

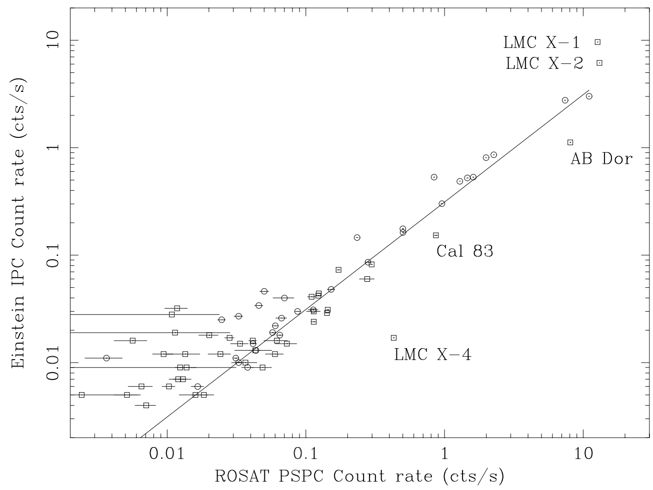

Fig. 1. Einstein IPC vs. ROSAT PSPC count rates. Sources identified with SNRs are marked with circles. The line is a linear fit to the SNR data points

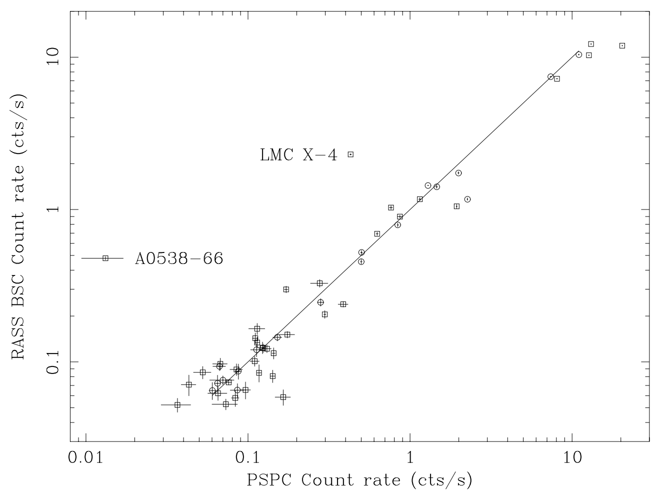

Fig. 2. ROSAT all-sky survey vs. PSPC pointing count rates. Circles mark SNRs which follow the line of equal count rates

3.3. Literature search with SIMBAD

To identify the PSPC sources with known objects we cross-correlated our catalogue with the SIMBAD data base operated at CDS. SIMBAD contains predominantly stars but also includes catalogues of sources from other wavelength bands together with references. This allows to define samples of sources with the same type (SNRs, SSSs, X-ray binaries, foreground stars and background objects) which can be used to classify the newly discovered sources using the global X-ray properties characteristic to the source class.

3.3.1. Supernova remnants

Table 6 lists 46 SNRs and candidates (indicated with SNR?) found in the literature and detected in ROSAT

PSPC pointings. Many of them were already seen by the Einstein IPC. The majority appears as extended X-ray sources with typical extent of 10″ − 40″. However the value can only be regarded as indicator for the extent because it is determined by a Gaussian approximation of the intensity profile. For sources with deviating profile the parameters determined by the ML algorithm become more and more unreliable. For this reason the count rates were re-determined for the sources already mentioned in Sect. 2.

From preliminary investigations of the PSPC catalogue Haberl et al. (1998) have shown that extent and likelihood for the extent (ML_{ext}) in combination with the hardness ratios can be used to characterize the class of SNRs. In Fig. 3 extent and ML_{ext} are plotted for all PSPC sources detected in the inner 18′ of the detector where the PSF of the instrument is best. The sources from Table 6 are marked with a square (filled for known SNRs and open for candidates; crossed squares for new candidates classified in this work – see below). The known X-ray binaries, SSS, foreground stars and AGN should be point sources and are marked with hexagons. On the left part of the diagram (left to the majority of unknown sources marked with a cross) many point sources appear with small extent. These are all detections with very good counting statistics (more than 400 counts) in which deviations of the PSF from the assumed Gaussian shape become significant, resulting in an artificial extent. This includes also most of the known SNRs which shows that the two parameters can only be used as indicator for source extent. Nevertheless the known SNRs are clearly distinguished showing the highest ML_{ext} values. For some of the SNR candidates found in the literature (mainly new candidates suggested by radio observations, Filipović et al. 1998) the source parameters derived from the PSPC observations support their classification. This is particularly true for PSPC source 712 which was detected by Einstein and suggested as SNR by WHHW91 (see Table 6). For source 687 source extent and hardness favour an SNR identification and the nearby foreground star proposed by Cowley et al. (1997) as optical counterpart for RX J0528.6 − 6836 is probably unrelated to the X-ray source. There is one unknown source (93) which is located in the area of the diagram where only SNRs are found. The hardness ratios are also compatible with such an interpretation. Other new sources with the highest ML_{ext} values, but below the majority of known SNRs, need to be investigated in detail as promising SNR candidates.

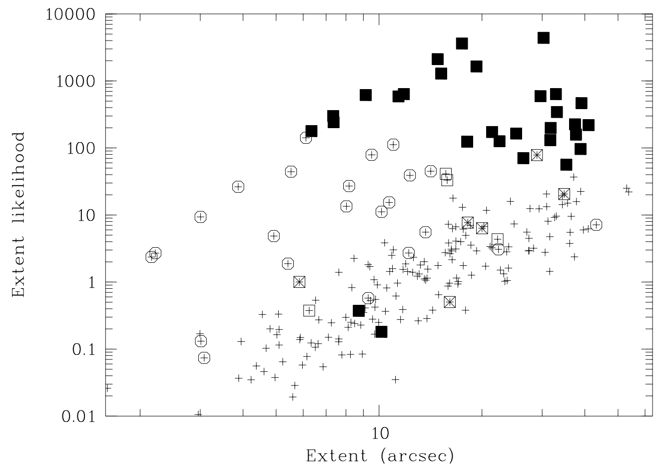

Fig. 3. Source extent and extent likelihood for PSPC sources with off-axis angle less than 18′ (crosses). SNRs are marked with squares (filled: secure, open: candidates, crossed: classified in this work) and known point sources (X-ray binaries, SSSs, stars and AGN) with hexagons

3.3.2. X-ray binaries and supersoft sources

X-ray binaries belong to the objects with hardest X-ray spectrum in the ROSAT energy band. From an investigation of the variability on time-scales of days to years of the PSPC sources presented in this work, HP99 proposed seven new candidates for X-ray binaries. Most of them are probably HMXBs and one is a candidate for a low mass X-ray binary (LMXB). The HMXB nature of one of them (source 1225, RX J0544.1 − 7100 = 1SAX J0544.1 − 710) was confirmed by the independent detection of X-ray pulses by the BeppoSAX satellite (Cusumano et al. 1998). Together with the previously known X-ray binaries their properties as determined from the PSPC observations are summarized in Table 7. It should be noted that the count rates (Col. 5) are only representative for a single observation. For more information on variability see HP99.

Supersoft sources were established as a new class of X-ray sources after the ROSAT discoveries of five new such objects. Before ROSAT only two (CAL 83 and CAL 87) were known from Einstein observations. SSSs are characterized by very soft X-ray spectra resulting in PSPC hardness ratios HR1 and HR2 close to −1.0. Foreground absorption may however increase HR1. HP99 proposed two new SSS candidates from their hardness ratios and X-ray variability. The properties of the known SSSs in the LMC which are all detected in PSPC observations are summarized in Table 7.

3.3.3. Background AGN and galaxies

Relatively few of the PSPC sources were identified with background objects like AGN and galaxies (Table 8), although many are expected from the $\log N - \log S$ distribution of extragalactic objects. Using a sensitivity of 6 10^{-3} cts s^{-1} for a typical 2000 s observation and the $\log N - \log S$ distribution from Hasinger et al. (1998), one would expect of the order of 5 background objects per square degree in LMC areas where the absorbing column density is 3 10^{21} cm^{-2} (e.g. Dickey et al. 1994). The PSPC observations cover in total an area of 58.6 square degrees, including areas where the absorption is only by the galactic contribution of about 6 10^{20} cm^{-2}. There the number of background objects can be up to 10 per square degree. Also large areas are covered by observations deeper than 2000 s, resulting in a lower limit of about 300 background objects expected in the catalogue.

Most of the known AGN were optically identified due to ROSAT follow-up observations of Einstein sources (e.g. Schmidtke et al. 1998). Three galaxies and a group of galaxies are proposed as optical counterparts from their positional coincidence. However, in these cases the error on the X-ray position is large and the identifications need to be confirmed as is also the case for source 1367.

3.3.4. Foreground stars

The source classes described so far contain bright X-ray sources which were in many cases already detected by X-ray instruments launched before ROSAT. Also ROSAT sources identified optically are already published. The high sensitivity of the ROSAT PSPC allowed for the first time to study the X-ray emission from normal stars. A large number of stars (mainly active corona late type stars) are therefore expected in the PSPC source catalogue in the direction of the LMC. Since many of these stars are detected in X-rays the first time, PSPC sources were "identified" with stars by correlation with the SIMBAD catalogue, i.e. by positional coincidence only. Few stars were identified by follow-up optical work published in the literature and six sources were proposed by HP99 as foreground stars from their X-ray spectral and temporal properties. In total up to 57 of the PSPC sources investigated in our fields correlate with foreground stars (Table 9). In 10 of these cases the identification is uncertain due to a large distance to the optical position and/or uncertain X-ray position.

A flux ratio $f_\mathrm{x}/f_\mathrm{opt}$ in the X-ray and optical band was calculated from the 0.1 − 2.4 keV count rate and optical magnitude m_GSC from the GSC from $\log(f_\mathrm{x}/f_\mathrm{opt}) = \log(\mathrm{PSPC\ counts/s}\ 10^{-11}) + 0.4 m_\mathrm{GSC} + 5.37$ (Maccacaro et al. 1988; Voges et al. 1999). We use here the more complete GSC instead of V or B magnitudes available for a smaller number of sources from the correlations with SIMBAD. A clear correlation of $f_\mathrm{x}/f_\mathrm{opt}$ with spectral type of the stars is seen with A and F stars as weakest X-ray emitters while dMe stars show highest $\log(f_\mathrm{x}/f_\mathrm{opt})$ values around −1.0 (Table 9).

3.4. Source classification

In Tables 6–9 in total 144 source "identifications" are summarized. In many cases these are based on optical identifications of previously known X-ray sources. Identifications from positional coincidence only (mainly foreground stars) are supported by their X-ray properties like hardness ratios and X-ray to optical flux ratios. In the following we investigate this sample of identified sources to find properties unique to the different types of X-ray emitters with the aim of a classification of the unidentified sources. Kahabka et al. (1999) have classified ROSAT PSPC sources in the Small Magellanic Cloud using hardness ratio criteria. Figure 4 (top) shows the hardness ratios of identified sources which have errors on both hardness ratios of less than 0.25. The different source classes occupy partially overlapping areas of the diagram. There are however parts of the parameter space where only sources from one class are found. SSSs exhibit HR2 below −0.70 and only foreground stars are found with HR2 $>$ −0.70 and HR1 $<$ 0.25. In the range HR1 $>$ 0.25 and −0.70 $<$ HR2 $<$ 0.25 only SNRs are located. In Fig. 4 (bottom) the hardness ratios of unidentified PSPC sources are drawn. The areas covered by different source classes are indicated by thick lines in both diagrams. Since most of the 758 PSPC sources have large error bars on the hardness ratios a restrictive selection was used to classify new sources. This yields a smaller number of sources, but maximizes the probability for giving the correct classification.

A more detailed classification requires the knowledge of foreground absorption to the sources. Because this varies across the LMC, sources with the same intrinsic X-ray spectrum are distributed over a range of hardness ratios, in particular HR1 which is most sensitive to absorption. The selection criteria used here are relatively insensitive to absorption. Only stars may be misclassified when higher absorption increases HR1 above 0.25.

Table 3 summarizes the selection criteria used to find new promising candidates for SNRs and SSSs in the LMC, foreground stars and background objects. The numbers of sources which obey the selection criteria (and not already included in a previous selection) are given in Col. 3. The number of finally classified sources are found in Col. 4. Sources on the hardness ratio dividing lines (error bar crossing the line) were included when the errors on HR1 (EHR1) and HR2 (EHR2) are both less than 0.25. As expected three of the HR-selected SNR candidates (153, 887 and 1293) are very likely identified with stars in the GSC, visible as bright point-like objects on the DSS images. These three were re-classified as foreground stars which is also consistent with their low $f_\mathrm{x}/f_\mathrm{opt}$ ratio (see below). One further HR-selected SNR candidate (327) was removed from the classification because it is located near the south ecliptic pole and far from the LMC. The classified sources are summarized in Table 10 and indicated by [SNR], [SSS] or [fg Star] in the remark column.

Supernova remnants are characterized by constant X-ray flux. The SNR candidates (from literature and from this work) were therefore investigated for temporal variability. In case of more than two PSPC detections a chi-square test against a constant count rate was performed as in HP99. The more appropriate hard band (0.5 − 2.0 keV)

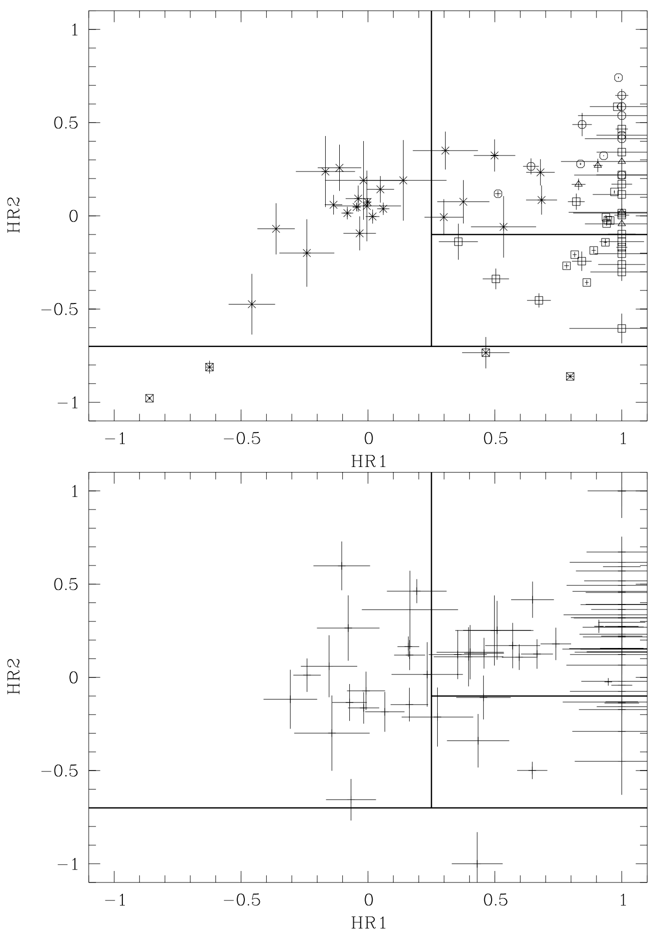

Fig. 4. Hardness ratios of known PSPC sources (top). X-ray binaries are marked with a hexagon, SSSs with crossed square, SNRs with square, stars with x, and AGN with triangle. The thick lines separate areas where only members of a single class are found. Hardness ratios of new PSPC sources with unknown nature (bottom). Only sources with error on HR1 and HR2 less than 0.25 are shown

was used. One case with clear variability was found for source 440 (probability more than 5 σ), which rules out the identification with an SNR. The detections of sources 93, 540, 712 and 1063 are consistent with constant flux, in agreement with their proposed SNR nature.

In the upper right part of Fig. 4 one finds all, stars, SNRs, AGN and X-ray binaries and it is not possible to classify the hard sources uniquely according to their hardness ratios. The very hard sources (HR1 > 0.75 and HR2 > -0.10) are candidates for either SNRs, AGN or X-ray binaries. Thirty-seven sources are classified as [hard] in Table 10. An inspection of the DSS images in the error circle of these hard sources reveals galaxy-like extended objects in three cases (101, 653 and 1184). All are located far from the LMC supplying further evidence that they are background objects unrelated to the LMC, in particular source 1184 is classified as AGN below. Also sources 418 and 1189 are located in areas where no LMC objects are expected. From the remaining hard sources many show empty error circles on the DSS images – at least those without indication of X-ray extent and position errors less than 20″. In three cases (482, 747 and 1181) even optical follow up observations failed to identify the optical counterpart (see Table 10). This suggests either background AGN or LMC objects optically too faint to be identified. If located in the LMC their PSPC count rates indicate typical X-ray luminosities of $10^{34} - 10^{35}$ erg s^{-1}, too high for cataclysmic variables, but consistent with LMXBs. The latter consist of a neutron star and a late type dwarf star, too faint for current optical instrumentation to be detected at the distance of the LMC, consistent with the empty error box. It is remarkable that most of these LMXB candidates are located around the optical bar of the LMC where also the SSSs are found. SSSs and LMXBs evolve from low-mass stars and belong to an older population compared to the HMXBs, many of which are found in areas of more recent star formation (e.g. in LMC4, HP99).

AGN and stars can be distinguished from their flux ratio $f_{\rm x}/f_{\rm opt}$ in the X-ray and optical band (e.g. Fig. 14 in Voges et al. 1999). Calculating $f_{\rm x}/f_{\rm opt}$ for a subsample of the PSPC catalogue with clear optical identifications and available visual or blue magnitudes (most from Schmidtke et al. 1994) yields similar results. $f_{\rm x}/f_{\rm opt}$ for some identified AGN, SSSs, X-ray binaries and foreground stars is shown in Fig. 5. The six identified AGN, gather near $\log(f_{\rm x}/f_{\rm opt}) = 0$ with HR1 above 0.8. However also SSSs and X-ray binaries can show high $f_{\rm x}/f_{\rm opt}$ ratio, even exceeding that of AGN. Stars have the lowest $f_{\rm x}/f_{\rm opt}$ and usually softer spectra (smaller HR1). For unidentified PSPC sources with a nearby GSC entry $f_{\rm x}/f_{\rm opt}$ was calculated using again the optical magnitude given in the GSC. The cases with error on HR1 of less than 0.25 are included in Fig. 5. Five sources with HR1 < 0.25 were not classified by criteria described above and show $\log(f_{\rm x}/f_{\rm opt}) < -0.5$, compatible with foreground stars. Two more candidates are found near identified foreground stars with HR1 < 0.75 and $\log(f_{\rm x}/f_{\rm opt}) < -2$. These seven sources are classified as [fg Star] in Table 10. Source 1163 with HR1 $= -1$ and low $f_{\rm x}/f_{\rm opt}$ (unusual for SSSs and also white dwarfs using examples from Thomas et al. 1998) is probably unrelated with the GSC entry as the GSC position is also outside the X-ray error circle.

Three unidentified PSPC sources exhibit HR1 > 0.25 and high $\log(f_{\rm x}/f_{\rm opt})$ above -1.0 (1, 37 and 1184). All three are located in the outermost regions of the 10° by 10° field covered by PSPC observations and are probably unrelated to the LMC. Source 1184, mentioned before to have a possible galaxy as likely optical counterpart, correlates as well as source 37 with a radio source. Based on the high $f_{\rm x}/f_{\rm opt}$ they are classified as [AGN] in Table 10. The three AGN candidates are relatively bright PSPC sources with two of them also detected in the RASS (1 and 37). Their optical brightness given in the GSC, range from 15.0

Table 3. Classification criteria

Source class	selection	unidentified sources	classified
SSS	$\mathrm{HR2} + \mathrm{EHR2} < -0.70$	3	3
fg star	$\mathrm{HR1} + \mathrm{EHR1} < 0.25$ $\mathrm{HR2} - \mathrm{EHR2} > -0.70$	12	
	$\mathrm{HR1} < 0.25$ $\mathrm{HR2} > -0.70$ $\mathrm{EHR1} < 0.25$ $\mathrm{EHR2} < 0.25$	5	
	$\mathrm{EHR1} < 0.25$ $-0.75 < HR1 < 0.25$ $\log(f_\mathrm{x}/f_\mathrm{opt}) < -0.5$	5	
	$\mathrm{EHR1} < 0.25$ $0.25 < HR1 < 0.75$ $\log(f_\mathrm{x}/f_\mathrm{opt}) < -1.0$	2	27
SNR	$\mathrm{ML}_\mathrm{ext} > 50$ offaxis angle $< 18'$	1	
	$\mathrm{HR1} - \mathrm{EHR1} > 0.25$ $\mathrm{HR2} - \mathrm{EHR2} > -0.70$ $\mathrm{HR2} + \mathrm{EHR2} < -0.10$	7	
	$\mathrm{HR1} > 0.25$ $-0.70 < \mathrm{HR2} < -0.10$ $\mathrm{EHR1} < 0.25$ $\mathrm{EHR2} < 0.25$	5	9
hard	$\mathrm{HR1} - \mathrm{EHR1} > 0.75$ $\mathrm{HR2} - \mathrm{EHR2} > -0.10$	35	
	$\mathrm{HR1} > 0.75$ $\mathrm{HR} > -0.10$ $\mathrm{EHR1} < 0.25$ $\mathrm{EHR2} < 0.25$	2	36
AGN	$\mathrm{EHR1} < 0.25$ $\mathrm{HR1} > 0.25$ $\log(f_\mathrm{x}/f_\mathrm{opt}) > -1.0$	3	3
stellar	$r_{90} < 20''$ distance to GSC entry $< r_{90}$	29	14

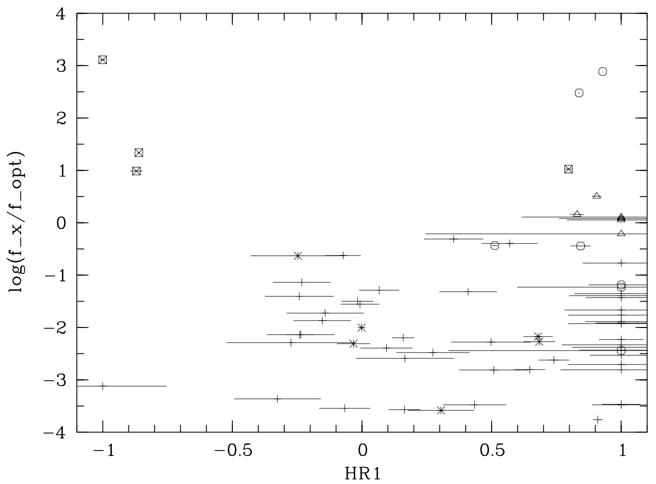

Fig. 5. Flux ratio $f_\mathrm{x}/f_\mathrm{opt}$ as function of hardness ratio 1. The optically identified sources are marked with different symbols (X-ray binaries: hexagon, SSSs: crossed square, foreground stars: x and AGN: triangle). Unidentified sources with error on HR1 less than 0.25 and nearby GSC entry are shown with HR1 error bars

to 15.3 mag. The majority of expected AGN in the PSPC catalogue is fainter and to find them by utilizing their $f_\mathrm{x}/f_\mathrm{opt}$ ratio more complete optical catalogues of the LMC area are required.

Additional PSPC sources likely related to foreground stars were obtained from the correlation with the GSC. A conservative selection of sources with position uncertainty r_{90} of less than $20''$ and a distance to GSC entries of less than r_{90} yields 29 objects. Removing unclear cases after visual investigation of the DSS images (several objects with similar brightness exist in the X-ray error circle) and objects with optical extent indicated in the GSC yields 16 stellar-like sources. Two of them are already classified as foreground stars from their low $f_\mathrm{x}/f_\mathrm{opt}$ ratio. The remaining 14 are classified as [stellar] in Table 10. In general this sample consists of X-ray fainter objects compared to the hardness ratio classified foreground stars (which have better photon statistics and therefore smaller errors on the hardness ratios). None of the 16 sources shows significant X-ray extent. However from their optical brightness – GSC magnitudes range from 10.1 to 14.8 mag – early type LMC stars not can be excluded (e.g. HMXBs in the LMC identified with Be stars have magnitudes at the lower end of the brightness distribution, cf. Haberl et al. 1997).

3.5. Source distribution

The spatial distribution of the 758 PSPC sources in the catalogue is shown in Fig. 6. The 144 identified sources from Tables 6–9 (including literature candidates) are marked according to their source class. In Fig. 7 the sources belonging to the LMC (SNRs, SSSs and X-ray binaries) are shown. Candidates and sources classified in this work are included. As was noted already by HP99 there is a significant concentration of X-ray binaries in and around the LMC4 supergiant shell. In contrast SSSs are only detected along the rim of the optical bar of the LMC. This includes all new SSS candidates from HP99 and this work, supporting their proposed nature. Many SSSs may be hidden inside the bar where the soft X-rays are strongly attenuated by photo-electric absorption.

4. Summary

The analysis of the ROSAT PSPC pointed data from 1990–1994 has yielded a catalogue of 758 discrete sources in an area of 58.6 square degrees. This is a factor of 3.5 more than found in the same area from the all-sky survey (Pietsch & Kahabka 1993) where the exposure quickly decreased with distance from the south ecliptic pole.

First cross-correlations with SIMBAD have resulted in about 140 identifications with objects of known nature partially only based on positional coincidence. The number of known objects in different source classes like SNRs, SSSs, X-ray binaries, foreground stars and background extragalactic objects are sufficiently high to derive criteria for a classification scheme. Using a preliminary

Fig. 6. Distribution of X-ray sources in the LMC region detected by the ROSAT PSPC (small circles). The source positions are plotted on a weak grey scale image ($0.1 - 2.4$ keV) for orientation. Identified sources are marked with different large symbols for different source classes; cross: SSS, square: SNR, circle: X-ray binary, cross + circle: foreground star, cross + square: background object

Fig. 7. Distribution of PSPC detected LMC sources: SNRs (square), SSSs (cross) and X-ray binaries (circle) including new candidates from this work. The background image is the same as in Fig. 6

scheme and additional information about time variability of sources in the PSPC catalogue Haberl & Pietsch (1999) already proposed several new candidates for X-ray binaries and supersoft sources in the LMC. In this paper a very restrictive hardness ratio classification scheme was used, resulting in promising new candidates for SNRs, SSS, X-ray binaries, background objects and foreground stars useful for follow-up studies to identify the X-ray sources.

Acknowledgements. The ROSAT project is supported by the German Bundesministerium für Bildung und Forschung (BMBF/DLR) and the Max-Planck-Gesellschaft. This research has made extensive use of the SIMBAD data base operated at CDS, Strasbourg, France.

References

Ardeberg A., Brunet J.P., Maurice E., Prevot L., 1972, A&AS 6, 249 (ABM72)
Chu Y.-H., 1997, AJ 113, 1815 (C97)
Chu Y.-H., Mac Low M.-M., Garcia-Segura G., Wakker B., Kennicutt C., 1993, ApJ 414, 213 (CMG93)
Chu Y.-H., Snowden S.L., 1998, AN 319, 101 (CS98)
Cowley A.P., Crampton D., Hutchings J.B., et al., 1984, ApJ 286, 196 (CCH84)
Cowley A.P., Schmidtke P.C., McGrath T.K., Ponder A.L., Fertig R.M., 1997, PASP 109, 21 (CSM97)
Crampton D., Gussie G., Cowley A.P., Schmidtke P.C., 1997, AJ 114, 2353 (CGC97)
Cusumano G., Mineo T., Nicastro L., Israel G.L., 1998, IAU Circ. 6861 (CMN98)
Dopita M.A., Bell J.F., Chu Y.-H., Lozinskaya T.A., 1994, ApJS 93, 455 (DBC94)
Davies R.D., Elliot K.H., Meaburn J., 1976, Mem. R. Astron. Soc. 81, 89 (DEM76)
Dickey J.M., Mebold U., Marx M., Amy S., Haynes R.F., Wilson W., 1994, A&A 289, 357
Downes R., Webbink R.F., Shara M.M., 1997, PASP 109, 345 (DWS97)
Filipović M.D., Haynes R.F., White G.L., et al., 1995, A&AS 111, 311
Filipović M.D., Pietsch W., Haynes R.F., et al., 1996, A&AS 127, 119
Filipović M.D., Haynes R.F., White G.L., Jones P.A., 1998, A&AS 130, 421 (FHW98)
Fehrenbach C., Duflot M., 1973, A&AS 10, 231 (FD73)
Gochermann J., Grothues H.-G., Östreicher M.O., Berghöfer T., Schmidt-Kaler Th., 1993, A&AS 99, 591 (GGO93)
Gurwell M., Hodge P., 1990, PASP 102, 849 (GH90)
Grothues H.-G., Östreicher M.O., Gochermann J., et al., 1997, A&AS 121, 247 (GOG97)
Haberl F., Dennerl K., Pietsch W., Reinsch K., 1997, A&A 318, 490
Haberl F., Pietsch W., 1998, Proceedings of the symposium "'Highlights in X-ray Astronomy in honour of Joachim Truemper's 65th birthday". Garching, June 1998
Haberl F., Pietsch W., 1999, A&A 344, 521 (HP99)
Haberl F., Pietsch W., Dennerl K., 1995, A&A 303, L49 (HPD95)
Haberl F., Pietsch W., Filipović M., 1998, in Proceedings of the IAU Symposium 190: New views of the Magellanic Clouds, PASP (in press)
Hasinger G., Burg R., Giacconi R., Schmidt M., Trümper J., Zamorani G., 1998, A&A 329, 482
Jaschek C., Jaschek M., Andrillat Y., Egret D., 1991, A&A 252, 229 (JJA91)
Kahabka P., Pietsch W., Filipović M.D., Haberl F., 1999, A&AS 136, 1
Lasker B.M., Sturch C.R., McLean B.J., et al., 1990, AJ 99, 2019
Long K.S., Helfand D.J., Grabelsky D.A., 1981, ApJ 248, 925 (LHG81)
Maccacaro T., Gioia I.M., Wolter A., Zamorani G., Stocke J.T., 1988, ApJ 326, 680
Mac Low M.-M., Chang T.H., Chu Y.-H., et al., 1998, ApJ 493, 260 (MCC98)
Moran E.C., Halpern J.P., Helfand D.J., 1996, ApJS 106, 341 (MHH96)
Olsen E.H., 1994, A&AS 106, 257 (O94)
Orio M., Della Valle M., Massone G., Ögelman H., 1997, A&A 325, L1 (O97)
Pfeffermann E., Briel U.G., Hippmann H., et al., 1986, Proc. SPIE 733, 519
Pietsch W., Kahabka P., 1993, in Lecture Notes in Physics 416: New Aspects of Magellanic Cloud Research, Baschek B., Klare G., Lequeux J. (eds.), p. 59
Pye J.P., McGale P.A., Allan D.J., et al., 1995, MNRAS 274, 1165 (PMA95)
Schmidtke P.C., Cowley A.P., Crane J.D., et al., 1998, astro-ph/9812217
Schmidtke P.C., Cowley A.P., Frattare L.M., et al., 1994, PASP 106, 843 (SCF94)
Smith R.C., Chu Y.-H., Mac Low M.-M., Oey M.S., Klein U., 1994, AJ 108, 1266 (SCL94)
Sanders D.B., Egami E., Lipari S., Mirabel I.F., Soifer B.T., 1995, AJ 110, 1993 (SEL95)
Snowden S.L., Petre R., 1994, ApJ 436, L123
Thomas H.-C., Beuermann K., Reinsch K., et al., 1998, A&A 335, 467
Trümper J., 1983, Adv. Space Res. 2, 241
Twarog B.A., 1980, ApJS 44, 1 (T80)
Voges W., Aschenbach B., Boller Th., et al., 1996, IAU Circ. 6420
Voges W., Aschenbach B., Boller Th., et al., 1999, A&A (in press)
Wang Q., Hamilton T., Helfand D.J., Wu X., 1991, ApJ 374, 475 (WHHW91)
Wang Q., Helfand D.J., 1991, ApJ 373, 497 (WH91)
White G.L., Batty M.J., Bunton J.D., Brown D.R., Corben J.B., 1987, MNRAS 227, 705 (WBB87)
White G.L., Bunton J.D., Anderson M.W.B., Batty M.J., Brown D.R., Corben J.B., 1991, MNRAS 248, 398 (WBA91)
Williams R.M., Chu Y.-H., Dickel J.R., et al., 1997, ApJ 480, 618 (WCD97)
Zimmermann H.U., Becker W., Belloni T., Döbereiner S., Izzo C., Kahabka P., Schwentker O., 1994, EXSAS User's Guide, MPE report, p. 257

Table 4. PSPC sources detected by the Einstein IPC

1	2	3	4	5	6	7	8
No	LHG	WHHW	d [″]	r_{90} [″]	PSPC count rate [cts s^{-1}]	IPC rate [cts s^{-1}]	Remarks
41	70		20.6	0.6	2.04e+01 ± 1.1e-01		HMXB LMC X-3
122	42	528.6-6529	6.8	0.6	8.07 ± 7.7e-02	1.121	foreground Star K0 (GGO93), AB Dor, HD 36705, (HP99)
180	39		15.3	7.2	3.13e-02 ± 1.3e-03	0.011	SNR DEM L 204 (LHG81)
219	34	525.3-6603	35.7	1.8	4.56e-01 ± 8.3e-03	0.488	SNR LHA 120-N 49B (WHHW91)
226	59	535.8-6604	26.2	2.4	7.39 ± 8.4e-02	2.766	SNR LHA 120-N 63A (WHHW91)
239	28	520.2-6607	35.4	8.5	1.42e-01 ± 4.9e-03	0.029	foreground Star G8V, (CCH84)
241	36	525.9-6608	14.0	1.0	2.06 ± 1.4e-02	0.861	SNR LHA 120-N 49 (WHHW91)
268	57	535.3-6614	36.0	31.3	3.35e-02 ± 4.9e-03	0.015	? fg Star dM4e (CCH84)
316	49	532.8-6624	8.7	0.6	4.30e-01 ± 5.5e-03	0.017	HMXB LMC X-4, HD269743 O8III, pulsar (HP99)
494		529.8-6716	29.4	12.3	4.87e-02 ± 7.9e-03	0.009	[stellar] GSC 8891.3619
538		526.1-6733	60.2	14.4	3.65e-03 ± 1.1e-03	0.011	SNR DEM L 192 (C97), or LMC W-R Star WC:, HD 36402 (DBC94)
540	48	532.5-6734	21.7	25.1	6.67e-02 ± 6.0e-03	0.026	SNR? 0532-67.5 (C97), RX J0532.5-6731 (ext. CSM97), const
542	14	509.6-6734	69.4	0.7	5.02e-01 ± 7.1e-03	0.163	SNR 0509.0-67.5 (WHHW91)
551	60	536.2-6737	25.4	38.2	8.99e-02 ± 1.3e-02	0.040	SNR DEM L 241 (C97), RX J0536.0-6735 variable (SCF94)
561		534.9-6741	46.3	45.1	6.18e-02 ± 1.2e-02	0.016	AGN RX J05348-6739, $z = 0.0720$ (CSM97)
562		532.3-6742	30.2	79.1	1.35e-02 ± 3.7e-03	0.012	
564		523.5-6744	31.9	20.8	1.30e-02 ± 1.9e-03	0.007	[SNR] no HRI detection by (CSM97)
592	10	505.9-6756	30.8	1.0	1.61 ± 2.0e-02	0.532	SNR DEM L 71 (WHHW91)
594		523.3-6756	58.0	10.0	3.55e-02 ± 2.5e-03	0.006	SNR in HII complex LHA 120-N 44 (shell 3 in CMG93)
603	31	522.5-6759	61.7	9.0	5.49e-02 ± 3.2e-03	0.034	SNR (s)? in HII complex LHA 120-N 44 (shell 1 in CMG93)
614	11	506.1-6806	21.6	1.1	9.57e-01 ± 1.6e-02	0.302	SNR LHA 120-N 23 (WHHW91)
634		518.8-6817	24.9	76.4	3.67e-02 ± 1.9e-02	0.010	
636	20	516.3-6819	19.3	27.2	1.10e-01 ± 7.2e-03	0.041	fg Star G1V (SCF94)
654	83	543.8-6823	37.0	8.5	8.66e-01 ± 3.0e-02	0.153	SSS CAL 83 (SCF94)
662	3		12.4	23.2	6.53e-03 ± 1.3e-03	0.006	
670	1	453.8-6834	24.9	1.7	5.00e-01 ± 6.7e-03	0.176	SNR 0453-68.5 (WHHW91)
686	86	546.6-6836	49.1	59.1	1.25e-02 ± 1.9e-02	0.009	RX J0546.3-6836 (no ID in SCF94)
687		528.8-6839	13.0	3.6	5.75e-02 ± 2.4e-03	0.019	SNR? B0528-6838 (FHW98), too hard for fg star G1V (CSM97)?
696	2	455.9-6844	8.1	7.2	4.16e-02 ± 2.1e-03	0.015	SNR LHA 120-N 86 (WHHW91)
707	13	509.3-6847	29.1	0.6	1.92 ± 1.7e-02	0.808	SNR LHA 120-N 103B (WHHW91), RX J0509.0-6844 (CSM97)
712	17	511.0-6848	33.5	4.9	3.27e-02 ± 2.4e-03	0.027	SNR? (WHHW91), const
742	6	459.1-6856	52.1	6.5	1.23e-01 ± 6.0e-03	0.042	foreground Star dMe, HD 268840 (CSM97)
747		547.4-6853	75.5	48.7	1.52e-02 ± 1.3e-02	0.028	[hard] RX J0547.0-6852 (no ID in SCF94)
749	43	529.7-6854	23.9	2.4	1.44e-01 ± 3.5e-03	0.031	foreground Star G2IV, HD 269620 (CSM97)
752	71	538.9-6855	23.8	1.2	2.98e-01 ± 4.8e-03	0.082	foreground Star G2V, RS CVn? (CSM97)
776	82	543.5-6901	43.2	26.9	2.44e-01 ± 8.4e-03	0.017	[SNR]
789	26	519.9-6905	5.9	0.7	1.46 ± 2.0e-02	0.523	SNR 0519-69.0 (WHHW91)
796	4	458.6-6909	45.7	16.4	2.85e-02 ± 2.2e-03	0.017	[hard]
813	15		29.0	21.4	1.18e-02 ± 2.2e-03	0.032	
826	67	538.1-6912	12.1	1.1	2.34e-01 ± 4.0e-03	0.146	SNR DEM L 263 (WHHW91), RX J0537.8-6911 (CSM97)
836	40	528.1-6915	20.5	21.8	4.37e-02 ± 1.3e-02	0.013	SNR 0528-69.2 (CS98)
840	62	536.8-6914	85.6	7.6	2.47e-02 ± 1.6e-03	0.025	SNR 30 Dor C, brightest knot in X-ray ring
863	25	519.8-6921	35.3	11.4	1.38e-02 ± 2.4e-03	0.009	no HRI detection by (SCF94)
866		536.2-6921	44.4	7.5	3.28e-02 ± 1.8e-03	0.010	SNR Honeycomb (CS98), RX J0535.8-6919 (CSM97)
877	79	540.6-6922	18.2	0.6	8.40e-01 ± 9.8e-03	0.532	SNR LHA 120-N 158A (CS98), 50ms PSR B0540-69
887	22		65.7	27.0	1.60e-02 ± 3.8e-03	0.005	[fg Star] GSC 9162.0126
902	69	538.7-6925	7.7	1.4	1.72e-01 ± 4.6e-03	0.073	foreground Star dMe (CSM97)
914		533.1-6928	17.0	6.5	1.84e-02 ± 3.3e-03	0.005	LMXB? (HP99)
915	27	520.1-6929	25.1	17.7	1.13e-01 ± 9.3e-03	0.031	SNR 0520-69.4 (WHHW91), RX J0519.8-6926 (SCF94)
943	19	514.0-6936	35.4	17.5	2.42e-02 ± 4.5e-03	0.012	foreground Star K1V (CSM97)
977	35	525.4-6942	5.3	1.1	7.37 ± 8.3e-02	3.008	SNR LHA 120-N 132D (WHHW91), RX J0525.0-6939 (CSM97)
978	23	519.1-6943	33.5	18.6	3.80e-02 ± 3.6e-03	0.009	SNR LHA 120-N 120 (WHHW91)
987	88	547.7-6943	74.1	4.9	5.02e-02 ± 3.7e-03	0.046	SNR DEM L 316 (WHHW91,CSM97), shell A (WCD97)

Table 4. continued

1	2	3	4	5	6	7	8
No	LHG	WHHW	d [″]	r_{90} [″]	PSPC count rate [cts s^{-1}]	IPC rate [cts s^{-1}]	Remarks
1001	78	540.1-6946	6.2	0.6	1.27e+01 ± 8.7e-02	9.632	HMXB LMC X-1
1024	93	553.0-6950	24.8	33.9	7.30e-02 ± 1.3e-02	0.015	[hard]
1036	92	551.6-6955	53.5	60.9	5.99e-02 ± 8.9e-03	0.012	foreground Star F5V:, HD 40156 (CSM97)
1040	16	509.8-6958	44.8	14.3	4.32e-02 ± 4.5e-03	0.013	AGN Sy1, $z = 0.175$ (WHHW91)
1043	53	534.5-6957	7.4	5.2	2.81e-01 ± 1.3e-02	0.086	SNR 0534-69.9 (CS98), RX J0534.0-6955 (CSM97)
1093	38	526.5-7014	4.0	3.7	4.14e-02 ± 2.7e-03	0.016	foreground Star K2IV-Vp, RS CVn (SCF94 HP99)
1094	32	524.6-7014	34.3	1.5	1.14e-01 ± 4.0e-03	0.024	AGN RXJ0524.0-7011 $z = 0.151$ (SCF94)
1136		554.1-7025	38.0	34.7	2.01e-02 ± 3.2e-03	0.018	no HRI detection by (CSM97)
1137	89	548.4-7026	9.8	5.8	1.52e-01 ± 9.6e-03	0.048	SNR 0548-70.4 (WHHW91)
1145	52	534.3-7029	6.0	7.0	7.06e-03 ± 1.2e-03	0.004	no HRI detection by (CSM97)
1147	18	513.5-7031	8.6	28.7	1.14e-01 ± 1.3e-02	0.030	foreground Star dM4e, V12567 (CCH84)
1160	54	534.9-7036	27.4	5.4	6.49e-02 ± 2.8e-03	0.018	SNR DEM L 238 (WHHW91), RX J0534.2-7034 (CSM97)
1164	97		67.2	19.2	5.64e-03 ± 1.5e-03	0.016	
1173	61	536.7-7040	16.9	4.9	6.02e-02 ± 2.7e-03	0.022	SNR DEM L 249 (WHHW91), RX J0536.1-7039 (CSM97)
1178	51		27.2	15.6	5.13e-03 ± 1.0e-03	0.005	
1181		536.7-7043	22.6	3.7	1.03e-02 ± 1.1e-03	0.006	[hard] RX J0536.0-7041 (no ID in CSM97)
1192	45	530.8-7049	24.0	41.6	2.44e-03 ± 4.0e-03	0.005	no HRI detection by (SCF94), no ID in (CCH84)
1222	47	532.6-7102	19.3	7.6	8.73e-02 ± 3.6e-03	0.030	SNR LHA 120-N 206 (WHHW91), RX J0531.9-7100 (SCF94)
1238	50		46.2	24.3	9.43e-03 ± 1.6e-03	0.012	
1240	87	547.5-7110	22.2	0.8	1.24e-01 ± 2.6e-03	0.044	SSS CAL 87
1242	33	524.8-7112	40.6	35.9	2.77e-01 ± 3.4e-02	0.060	foreground Star dM5e (CCH84)
1279	46	532.3-7132	82.0	66.4	1.44e-02 ± 1.7e-02	0.019	AGN RXJ0531.5-7130 $z = 0.2214$ (SCF94)
1308		517.4-7149	22.6	17.2	1.20e-02 ± 1.7e-03	0.007	RX J0516.7-7146 (no ID in CSM97)
1325	30	521.3-7201	16.3	0.6	1.31e+01 ± 3.2e-02	6.154	LMXB LMC X-2

Notes to the remark column to this and following tables:
Abbreviations for references given in parenthesis are described in the literature list,
Unsecure identifications from positional uncertainty begin with? in the remark,
Candidates from literature are marked with? after source class name,
Abbreviations:
SEP: in pointing near south ecliptic pole,
GSC: HST guide star catalogue (Lasker et al. 1990),
NED: NASA/IPAC extragalactic database, operated by the Jet Propulsion Laboratory, California Institute, of Technology, under contract with the National Aeronautics and Space Administration,
fg: foreground, var: X-ray variable, const: X-ray constant.

Table 5. PSPC sources detected in the ROSAT all-sky survey

1	2	3	4	5	6	7	8
No	BSC name	d [″]	r_{90} [″]	r_{BSC} [″]	PSPC count rate [cts s^{-1}]	BSC rate [cts s^{-1}]	Remarks
1	1RXS J054026.6-624100	44.4	44.9	8	1.65e-01 ± 1.8e-02	5.87e-02 ± 6.9e-03	[AGN]
37	1RXS J055225.0-640206	25.6	43.1	7	1.75e-01 ± 1.9e-02	1.51e-01 ± 7.5e-03	[AGN] PMNJ0552-6401
41	1RXS J053855.5-640457	16.8	0.6	6	2.04e+01 ± 1.1e-01	1.19e+01 ± 7.9e-02	HMXB LMC X-3
54	1RXS J054641.2-641513	12.6	23.4	7	3.87e-01 ± 2.7e-02	2.39e-01 ± 1.0e-02	QSO PMN J0546-6415, $z = 0.323000$ (NED)
61	1RXS J054333.4-642252	10.9	24.6	7	6.53e-02 ± 8.8e-03	6.22e-02 ± 6.4e-03	fg Star? (HP99)
93	1RXS J053724.2-650413	10.2	11.5	14	8.61e-02 ± 8.4e-03	6.52e-02 ± 6.8e-03	[SNR] GSC 8887.0518, GSC-ext, const
101	1RXS J054139.1-651117	19.0	32.8	16	8.61e-02 ± 7.5e-03	8.92e-02 ± 7.9e-03	[hard] Galaxy? (DSS)
122	1RXS J052844.7-652700	1.8	0.6	6	8.07 ± 7.7e-02	7.22 ± 4.3e-02	foreground Star K0 (GGO93), AB Dor, HD 36705, (HP99)
131	1RXS J053555.0-653039	9.3	13.0	7	1.31e-01 ± 8.1e-03	1.22e-01 ± 7.2e-03	HMXB? (HP99)
219	1RXS J052522.7-655923	42.3	1.8	0	4.56e-01 ± 8.3e-03	1.44 ± 0.0	SNR LHA 120-N 49B (WHHW91)
226	1RXS J053544.0-660212	8.8	2.4	6	7.39 ± 8.4e-02	7.45 ± 4.2e-02	SNR LHA 120-N 63A (WHHW91)
239	1RXS J052013.8-660423	4.5	8.5	7	1.42e-01 ± 4.9e-03	8.07e-02 ± 7.6e-03	foreground Star G8V, (CCH84)
241	1RXS J052559.2-660450	23.6	1.0	6	2.06 ± 1.4e-02	1.17 ± 2.2e-02	SNR LHA 120-N 49 (WHHW91)
273	1RXS J051957.5-661357	0.7	15.8	9	8.35e-02 ± 4.5e-03	5.80e-02 ± 7.1e-03	foreground Star G5, HD 269339 (GOG97)
311	1RXS J060755.1-662136	9.7	20.3	6	7.60e-02 ± 3.3e-03	7.34e-02 ± 2.8e-03	[fg Star] GSC 8905.0616, SEP
316	1RXS J053246.1-662203	22.4	0.6	6	4.30e-01 ± 5.5e-03	2.30 ± 2.4e-02	HMXB LMC X-4, HD269743 O8III, pulsar (HP99)
380	1RXS J050304.8-663345	12.4	9.0	9	1.17e-01 ± 3.7e-03	8.47e-02 ± 1.1e-02	AGN RXJ0503.1-6634 $z = 0.064$ (SCF94), CAL F, (HP99)
434	1RXS J051827.2-665122	25.8	33.4	7	6.75e-02 ± 7.0e-03	9.70e-02 ± 8.8e-03	
436	1RXS J053539.0-665158	15.5	9.8	6	1.32e-02 ± 3.8e-03	4.79e-01 ± 1.2e-02	HMXB Be/X transient A0538-66, pulsar (HP99)
540	1RXS J053226.8-673115	14.2	25.1	9	6.67e-02 ± 6.0e-03	9.34e-02 ± 6.0e-03	SNR? 0532-67.5 (C97), RX J0532.5-6731 (ext. CSM97), const
542	1RXS J050930.8-673116	5.5	0.7	6	5.02e-01 ± 7.1e-03	5.22e-01 ± 1.7e-02	SNR 0509.0-67.5 (WHHW91)
551	1RXS J053602.3-673502	33.0	38.2	8	8.99e-02 ± 1.3e-02	7.59e-02 ± 5.0e-03	SNR DEM L 241 (C97), RX J0536.0-6735 variable (SCF94)
628	1RXS J043950.4-680854	15.7	1.3	6	1.15 ± 2.1e-02	1.17 ± 2.7e-02	SSS RXJ0439.8-6809, 1ES 0439-682
634	1RXS J051833.2-681328	38.3	76.4	8	3.67e-02 ± 1.9e-02	5.22e-02 ± 5.5e-03	
636	1RXS J051607.1-681538	12.5	27.2	7	1.10e-01 ± 7.2e-03	1.01e-01 ± 7.5e-03	fg Star G1V (SCF94)
653	1RXS J043612.5-682236	22.5	29.8	15	5.26e-02 ± 6.5e-03	8.53e-02 ± 8.0e-03	[hard] Galaxy? (DSS)
654	1RXS J054334.5-682218	14.7	8.5	6	8.66e-01 ± 3.0e-02	8.99e-01 ± 1.9e-02	SSS CAL 83 (SCF94)
670	1RXS J045338.0-682917	8.7	1.7	7	5.00e-01 ± 6.7e-03	4.55e-01 ± 1.6e-02	SNR 0453-68.5 (WHHW91)
707	1RXS J050859.1-684331	3.4	0.6	6	1.92 ± 1.7e-02	1.74 ± 3.5e-02	SNR LHA 120-N 103B (WHHW91), RX J0509.0-6844 (CSM97)
742	1RXS J045844.9-685048	10.7	6.5	8	1.23e-01 ± 6.0e-03	1.24e-01 ± 1.1e-02	foreground Star dMe, HD 268840 (CSM97)
749	1RXS J052926.6-685159	5.4	2.4	8	1.44e-01 ± 3.5e-03	1.14e-01 ± 9.7e-03	foreground Star G2IV, HD 269620 (CSM97)
752	1RXS J053834.8-685305	2.7	1.2	7	2.98e-01 ± 4.8e-03	2.05e-01 ± 1.2e-02	foreground Star G2V, RS CVn? (CSM97)
789	1RXS J051934.7-690202	6.7	0.7	6	1.46 ± 2.0e-02	1.41 ± 3.2e-02	SNR 0519-69.0 (WHHW91)
877	1RXS J054011.5-692011	18.6	0.6	7	8.40e-01 ± 9.8e-03	7.92e-01 ± 2.1e-02	SNR LHA 120-N 158A (CS98), 50ms PSR B0540-69
902	1RXS J053815.7-692337	8.5	1.4	11	1.72e-01 ± 4.6e-03	2.99e-01 ± 1.5e-02	foreground Star dMe (CSM97)
915	1RXS J051944.2-692551	30.0	17.7	11	1.13e-01 ± 9.3e-03	1.20e-01 ± 1.2e-02	SNR 0520-69.4 (WHHW91), RX J0519.8-6926 (SCF94)
977	1RXS J052502.8-693840	16.1	1.1	6	7.37 ± 8.3e-02	1.04e+01 ± 8.6e-02	SNR LHA 120-N 132D (WHHW91), RX J0525.0-6939 (CSM97)
1001	1RXS J053938.8-694515	34.9	0.6	6	1.27e+01 ± 8.7e-02	1.03e+01 ± 6.6e-02	HMXB LMC X-1
1024	1RXS J055230.8-694910	7.1	33.9	8	7.30e-02 ± 1.3e-02	5.27e-02 ± 4.3e-03	[hard]
1030	1RXS J051351.2-695145	2.3	1.1	6	1.94 ± 1.7e-02	1.05 ± 3.3e-02	SSS RXJ0513.9-6951, HV5682, (HP99)
1039	1RXS J052749.6-695412	7.2	2.8	8	1.11e-01 ± 4.5e-03	1.43e-01 ± 1.2e-02	SSS RXJ0527.8-6954, (HP99)
1040	1RXS J050915.6-695413	11.0	14.3	8	4.32e-02 ± 4.5e-03	7.09e-02 ± 1.1e-02	AGN Sy1, $z = 0.175$ (WHHW91)
1043	1RXS J053401.3-695519	18.6	5.2	9	2.81e-01 ± 1.3e-02	2.46e-01 ± 1.4e-02	SNR 0534-69.9 (CS98), RX J0534.0-6955 (CSM97)
1094	1RXS J052402.0-701108	4.0	1.5	7	1.14e-01 ± 4.0e-03	1.34e-01 ± 1.1e-02	AGN RXJ0524.0-7011 $z = 0.151$ (SCF94)
1137	1RXS J054748.8-702454	6.7	5.8	8	1.52e-01 ± 9.6e-03	1.45e-01 ± 7.8e-03	SNR 0548-70.4 (WHHW91)
1147	1RXS J051302.1-702742	6.5	28.7	8	1.14e-01 ± 1.3e-02	1.65e-01 ± 1.4e-02	foreground Star dM4e, V12567 (CCH84)
1160	1RXS J053414.3-703401	21.0	5.4	18	6.49e-02 ± 2.8e-03	7.23e-02 ± 9.5e-03	SNR DEM L 238 (WHHW91), RX J0534.2-7034 (CSM97)
1173	1RXS J053604.1-703925	43.5	4.9	15	6.02e-02 ± 2.7e-03	6.49e-02 ± 8.4e-03	SNR DEM L 249 (WHHW91), RX J0536.1-7039 (CSM97)
1222	1RXS J053158.4-710036	25.8	7.6	15	8.73e-02 ± 3.6e-03	8.68e-02 ± 1.0e-02	SNR LHA 120-N 206 (WHHW91), RX J0531.9-7100 (SCF94)
1240	1RXS J054648.3-710924	32.4	0.8	8	1.24e-01 ± 2.6e-03	1.23e-01 ± 7.9e-03	SSS CAL 87
1242	1RXS J052402.6-710956	19.6	35.9	7	2.77e-01 ± 3.4e-02	3.28e-01 ± 1.9e-02	foreground Star dM5e (CCH84)
1316	1RXS J054959.9-715158	40.5	7.0	6	6.27e-01 ± 9.2e-03	6.93e-01 ± 1.7e-02	SSS RXJ0550.0-7151
1325	1RXS J052027.6-715755	25.5	0.6	6	1.31e+01 ± 3.2e-02	1.22e+01 ± 1.0e-01	LMXB LMC X-2
1334	1RXS J061828.8-720242	25.8	9.1	6	7.63e-01 ± 1.8e-02	1.03 ± 3.0e-02	foreground Star K3:V:, HD 45081, 2RE J0618-720 (PMA95)
1350	1RXS J061132.6-721335	6.2	26.8	10	9.66e-02 ± 7.0e-03	6.54e-02 ± 8.4e-03	[fg Star] GSC 9172.1315

Table 6. SNRs and candidates in the LMC

1	2	3	4	5	6	7	8	9	10
No	RA (J2000.0)	Dec (J2000.0)	r_{90} [″]	Count Rate [cts s^{-1}]	HR1	HR2	Extent [″]	ML_{ext}	Remarks
180	05 27 52.4	−65 49 30	7.2	3.13e-02 ± 1.3e-03	0.67 ± 0.05	−0.45 ± 0.04	41.0	219.4	SNR DEM L 204 (LHG81)
219	05 25 29.3	−65 59 35	1.8	4.56e-01 ± 8.3e-03	0.94 ± 0.01	−0.14 ± 0.02	19.3	1647.5	SNR LHA 120-N 49B (WHHW91)
226	05 35 45.1	−66 02 06	2.4	7.39 ± 8.4e-02	0.94 ± 0.00	−0.01 ± 0.01	28.5	353.0	SNR LHA 120-N 63A (WHHW91)
241	05 26 01.9	−66 05 07	1.0	2.06 ± 1.4e-02	0.95 ± 0.00	−0.02 ± 0.01	11.4	588.1	SNR LHA 120-N 49 (WHHW91)
326	05 01 53.0	−66 25 08	9.8	2.43e-03 ± 6.5e-04	1.00 ± 0.49	1.00 ± 0.36	6.2	0.4	SNR? B0501-6629 (FHW98)
329	04 54 49.3	−66 25 35	4.8	2.74e-02 ± 1.4e-03	0.84 ± 0.04	−0.24 ± 0.05	22.5	125.8	SNR LHA 120-N 11L (MCC98)
345	04 56 46.2	−66 28 27	12.2	1.36e-02 ± 1.3e-03	1.00 ± 0.21	−1.00 ± 1.20	38.9	96.5	SNR (s)? in HII complex LHA 120-N 11, central shell (MCC98)
402	05 37 04.2	−66 40 08	64.5	6.85e-03 ± 1.1e-02			49.3	1.8	SNR? DEM L 255 (DEM76)
440	05 29 59.3	−66 53 13	13.2	1.25e-02 ± 3.7e-03	1.00 ± 3.43	1.00 ± 6.74	0.0	0.0	SNR? B0530-6655 (FHW98), var
447	04 53 16.8	−66 54 34	43.7	5.37e-02 ± 4.4e-03	1.00 ± 0.21	−0.60 ± 0.08	104.2	13.1	SNR RX J0453.1-6655 near N4D (SCL94)
493	04 54 28.3	−67 12 32	4.6	2.99e-02 ± 1.7e-03	0.50 ± 0.05	−0.34 ± 0.06	21.4	173.1	SNR RX J0454.5-6713 near N9 (SCL94)
498	05 28 16.2	−67 14 17	29.3	9.62e-03 ± 2.8e-03	1.00 ± 2.56		0.0	0.0	SNR B0528-6716 (FHW98)
510	05 09 43.7	−67 16 33	24.7	3.44e-03 ± 4.6e-03	1.00 ± 0.60	1.00 ± 1.99	22.2	4.3	SNR? B0509-6720 (FHW98)
538	05 26 04.6	−67 30 00	14.4	3.65e-03 ± 1.1e-03	1.00 ± 0.52	1.00 ± 1.39	8.7	0.4	SNR DEM L 192 (C97), or LMC W-R Star WC:, HD 36402 (DBC94)
540	05 32 24.4	−67 31 10	25.1	6.67e-02 ± 6.0e-03	1.00 ± 0.49	−0.45 ± 0.09	32.6	1.3	SNR? 0532-67.5 (C97), RX J0532.5-6731 (ext. CSM97), const
542	05 09 31.7	−67 31 18	0.7	5.02e-01 ± 7.1e-03	0.78 ± 0.01	−0.27 ± 0.01	9.1	616.6	SNR 0509.0-67.5 (WHHW91)
551	05 36 01.7	−67 34 29	38.2	8.99e-02 ± 1.3e-02	1.00 ± 0.11	0.11 ± 0.14	56.6	6.4	SNR DEM L 241 (C97), RX J0536.0-6735 variable (SCF94)
592	05 05 42.7	−67 52 40	1.0	1.61 ± 2.0e-02	0.81 ± 0.01	−0.21 ± 0.01	17.5	3622.9	SNR DEM L 71 (WHHW91)
594	05 23 01.0	−67 53 08	10.0	3.55e-02 ± 2.5e-03	1.00 ± 0.04	0.17 ± 0.06	37.7	158.3	SNR in HII complex LHA 120-N 44 (shell 3 in CMG93)
603	05 22 17.3	−67 57 25	9.0	5.49e-02 ± 3.2e-03	1.00 ± 0.03	0.00 ± 0.06	37.4	225.2	SNR (s)? in HII complex LHA 120-N 44 (shell 1 in CMG93)
614	05 05 55.8	−68 01 47	1.1	9.57e-01 ± 1.6e-02	0.89 ± 0.01	−0.19 ± 0.02	15.2	1288.0	SNR LHA 120-N 23 (WHHW91)
670	04 53 37.3	−68 29 25	1.7	5.00e-01 ± 6.7e-03	0.86 ± 0.01	−0.36 ± 0.01	30.3	4395.5	SNR 0453-68.5 (WHHW91)
687	05 28 31.6	−68 36 14	3.6	5.75e-02 ± 2.4e-03	1.00 ± 0.19	0.01 ± 0.05	15.8	33.0	SNR? B0528-6838 (FHW98), too hard for fg star G1V (CSM97)?
696	04 55 44.3	−68 39 03	7.2	4.16e-02 ± 2.1e-03	1.00 ± 0.12	−0.30 ± 0.05	39.1	466.0	SNR LHA 120-N 86 (WHHW91)
707	05 08 59.3	−68 43 34	0.6	1.92 ± 1.7e-02	0.97 ± 0.00	0.13 ± 0.01	7.3	300.1	SNR LHA 120-N 103B (WHHW91), RX J0509.0-6844 (CSM97)
712	05 10 48.9	−68 45 27	4.9	3.27e-02 ± 2.4e-03	1.00 ± 0.10	0.34 ± 0.07	15.7	41.1	SNR? (WHHW91), const
789	05 19 34.9	−69 02 09	0.7	1.46 ± 2.0e-02	0.95 ± 0.00	−0.02 ± 0.01	7.4	241.7	SNR 0519-69.0 (WHHW91)
826	05 37 46.8	−69 10 10	1.1	2.34e-01 ± 4.0e-03	1.00 ± 0.02	0.47 ± 0.02	11.8	637.5	SNR DEM L 263 (WHHW91), RX J0537.8-6911 (CSM97)
835	05 13 13.5	−69 11 30	38.7	1.41e-02 ± 2.8e-03	1.00 ± 0.42	−0.34 ± 0.17	0.0	0.0	SNR B0513-6915 (FHW98)
836	05 27 43.4	−69 11 50	21.8	4.37e-02 ± 1.3e-02	1.00 ± 0.74	1.00 ± 6.84	10.2	0.2	SNR 0528-69.2 (CS98)
840	05 36 18.1	−69 12 58	7.6	2.47e-02 ± 1.6e-03	0.89	0.11	31.7	130.6	SNR 30 Dor C, brightest knot in X-ray ring
854	05 35 28.8	−69 16 16	7.5	4.38e-03 ± 8.3e-04	1.00 ± 0.27	0.21 ± 0.20	0.0	0.0	SNR SN1987A
866	05 35 45.8	−69 18 10	7.5	3.28e-02 ± 1.8e-03	1.00 ± 0.09	−0.14 ± 0.05	31.8	199.1	SNR Honeycomb (CS98), RX J0535.8-6919 (CSM97)
877	05 40 10.9	−69 19 53	0.6	8.40e-01 ± 9.8e-03	0.98 ± 0.00	0.58 ± 0.01	6.3	178.8	SNR LHA 120-N 158A (CS98), 50ms PSR B0540−69
915	05 19 47.4	−69 26 15	17.7	1.13e-01 ± 9.3e-03	0.36 ± 0.08	−0.14 ± 0.10	41.5	15.4	SNR 0520-69.4 (WHHW91), RX J0519.8-6926 (SCF94)
924	05 39 31.1	−69 27 31	13.5	3.10e-02 ± 3.3e-03	0.98	−0.29	35.3	56.3	SNR DEM L 269 (C97)
977	05 25 02.9	−69 38 56	1.1	7.37 ± 8.3e-02	0.94 ± 0.00	−0.04 ± 0.01	14.8	2110.5	SNR LHA 120-N 132D (WHHW91), RX J0525.0-6939 (CSM97)
978	05 18 43.4	−69 39 10	18.6	3.80e-02 ± 3.6e-03	1.00 ± 0.29	−0.31 ± 0.09	39.6	11.7	SNR LHA 120-N 120 (WHHW91)
987	05 47 20.9	−69 41 27	4.9	5.02e-02 ± 3.7e-03	1.00 ± 0.10	0.22 ± 0.07	18.1	124.1	SNR DEM L 316 (WHHW91,CSM97), shell A (WCD97)
993	05 46 55.3	−69 42 53	9.3	4.54e-02 ± 3.6e-03	0.95	0.21	26.4	70.5	SNR DEM L 316, shell B (WCD97)
1043	05 34 03.2	−69 55 03	5.2	2.81e-01 ± 1.3e-02	1.00 ± 0.11	−0.20 ± 0.05	32.9	636.4	SNR 0534-69.9 (CS98), RX J0534.0-6955 (CSM97)
1137	05 47 49.0	−70 24 47	5.8	1.52e-01 ± 9.6e-03	1.00 ± 0.05	−0.10 ± 0.06	25.2	164.3	SNR 0548-70.4 (WHHW91)
1160	05 34 14.8	−70 33 40	5.4	6.49e-02 ± 2.8e-03	0.82 ± 0.03	0.08 ± 0.04	33.1	344.4	SNR DEM L 238 (WHHW91), RX J0534.2-7034 (CSM97)
1167	05 27 44.9	−70 36 16	57.8	1.74e-02 ± 3.5e-03	1.00 ± 0.66	1.00 ± 0.33	57.7	3.7	SNR? DEM L 208 (DEM76)
1173	05 36 05.3	−70 38 42	4.9	6.02e-02 ± 2.7e-03	1.00 ± 0.02	−0.17 ± 0.04	29.7	591.9	SNR DEM L 249 (WHHW91), RX J0536.1-7039 (CSM97)
1222	05 31 56.2	−71 00 12	7.6	8.73e-02 ± 3.6e-03	1.00 ± 0.09	−0.26 ± 0.04	43.3	138.1	SNR LHA 120-N 206 (WHHW91), RX J0531.9-7100 (SCF94)

Table 7. X-ray binaries and supersoft sources in the LMC

1	2	3	4	5	6	7	8
No	RA	Dec	r_{90}	Count Rate	HR1	HR2	Remarks
	(J2000.0)		[″]	[cts s^{-1}]			
41	05 38 56.8	−64 05 12	0.6	2.04e+01 ± 1.1e-01	0.84 ± 0.00	0.28 ± 0.01	HMXB LMC X-3
106	05 31 35.3	−65 18 03	18.8	2.49e-02 ± 1.6e-03	1.00 ± 0.39	0.23 ± 0.06	HMXB? (HP99)
131	05 35 53.7	−65 30 34	13.0	1.31e-01 ± 8.1e-03	1.00 ± 0.19	0.22 ± 0.06	HMXB? (HP99)
137	05 32 25.2	−65 35 09	17.4	7.09e-03 ± 1.8e-03	1.00 ± 1.14	1.00 ± 1.39	HMXB? (HP99)
184	05 32 32.0	−65 51 42	3.3	1.11e-02 ± 6.3e-04	1.00 ± 0.10	0.43 ± 0.05	HMXB OB variable RXJ0532.5-6551, Sk −65 66 (HPD95 HP99)
204	05 29 48.2	−65 56 44	2.8	2.43e-01 ± 1.6e-02	0.84 ± 0.04	0.49 ± 0.06	HMXB Be/X transient RXJ0529.8-6556, pulsar (HP99)
252	05 31 12.8	−66 07 03	2.2	5.34e-01 ± 2.1e-02	0.64 ± 0.03	0.27 ± 0.04	HMXB Be/X transient EXO053109-6609, pulsar (HP99)
316	05 32 49.5	−66 22 12	0.6	4.30e-01 ± 5.5e-03	0.51 ± 0.01	0.12 ± 0.02	HMXB LMC X-4, HD269743 O8III, pulsar (HP99)
331	05 02 54.7	−66 26 00	38.0	3.23e-03 ± 8.1e-04	1.00 ± 0.67	0.43 ± 0.18	HMXB Be/X transient RXJ0502.9-6626, pulsar (SCF94)
436	05 35 41.6	−66 51 58	9.8	1.32e-02 ± 3.8e-03	1.00 ± 0.40	0.23 ± 0.28	HMXB Be/X transient A0538-66, pulsar (HP99)
462	05 35 05.9	−67 00 15	4.0	6.38e-02 ± 7.2e-03	1.00 ± 0.15	0.41 ± 0.11	HMXB? (HP99)
513	05 12 41.8	−67 17 22	4.0	1.31e-02 ± 1.4e-03	1.00 ± 0.17	0.54 ± 0.10	HMXB? (HP99)
914	05 32 45.1	−69 26 15	6.5	1.84e-02 ± 3.3e-03	1.00 ± 0.31	0.29 ± 0.19	LMXB? (HP99)
946	05 20 30.4	−69 32 03	16.6	4.83e-02 ± 4.0e-03	1.00 ± 0.13	0.59 ± 0.07	HMXB? RXJ0520.5-6932, O8e (SCF94), (HP99)
1001	05 39 40.3	−69 44 41	0.6	1.27e+01 ± 8.7e-02	0.99 ± 0.00	0.74 ± 0.00	HMXB LMC X-1
1225	05 44 06.2	−71 00 50	3.3	4.41e-02 ± 2.0e-03	1.00 ± 0.03	0.65 ± 0.03	HMXB RX J0544.1-7100 (HP99), pulsar (CMN98)
1325	05 20 29.4	−71 57 31	0.6	1.31e+01 ± 3.2e-02	0.93 ± 0.00	0.32 ± 0.00	LMXB LMC X-2
569	05 07 08.8	−67 43 28	18.7	9.33e-03 ± 1.6e-03	−1.00 ± 2.12		SSS? (HP99)
628	04 39 47.9	−68 09 02	1.3	1.15 ± 2.1e-02	−1.00 ± 0.01		SSS RXJ0439.8-6809, 1ES 0439-682
654	05 43 36.7	−68 22 26	8.5	8.66e-01 ± 3.0e-02	−0.87 ± 0.02	−1.00 ± 0.51	SSS CAL 83 (SCF94)
782	04 54 01.8	−69 00 34	11.4	9.49e-01 ± 9.4e-02	0.46 ± 0.09	−0.73 ± 0.08	SSS? (HP99)
1030	05 13 51.5	−69 51 46	1.1	1.94 ± 1.7e-02	−0.86 ± 0.00	−0.98 ± 0.01	SSS RXJ0513.9-6951, HV5682, (HP99)
1039	05 27 48.6	−69 54 07	2.8	1.11e-01 ± 4.5e-03	−1.00 ± 0.01		SSS RXJ0527.8-6954, (HP99)
1161	05 37 44.0	−70 33 50	17.2	3.53e-03 ± 8.4e-04	−1.00 ± 0.33		SSS or foreground WD? RXJ0537.7-7034 (O97, HP99)
1240	05 46 46.3	−71 08 53	0.8	1.24e-01 ± 2.6e-03	0.80 ± 0.01	−0.86 ± 0.01	SSS CAL 87
1316	05 50 03.2	−71 51 21	7.0	6.27e-01 ± 9.2e-03	−0.62 ± 0.01	−0.81 ± 0.03	SSS RXJ0550.0-7151

Table 8. Identification with background AGN and galaxies

1	2	3	4	5	6	7	8
No	RA	Dec	r_{90}	Count Rate	HR1	HR2	Remarks
	(J2000.0)		[″]	[cts s^{-1}]			
44	05 32 29.9	−64 06 41	75.6	1.19e-02 ± 1.4e-02	1.00 ± 0.74		? Galaxy group AM 0532-640 (NED)
54	05 46 40.0	−64 15 02	23.4	3.87e-01 ± 2.7e-02	0.67 ± 0.06	0.13 ± 0.08	QSO PMN J0546-6415, z=0.323000 (NED)
100	05 15 10.9	−65 11 31	72.4	1.14e-02 ± 2.8e-03	1.00 ± 0.75	1.00 ± 1.68	? Galaxy 051505-6513 (GH90)
380	05 03 02.7	−66 33 43	9.0	1.17e-01 ± 3.7e-03	0.83 ± 0.03	0.17 ± 0.03	AGN RXJ0503.1-6634 z=0.064 (SCF94), CAL F, (HP99)
411	04 54 11.3	−66 43 27	11.3	2.69e-02 ± 2.0e-03	1.00 ± 0.24	0.29 ± 0.07	AGN RX J0454.1-6643, z=0.2279 (CGC97)
433	06 07 41.0	−66 51 37	46.3	1.68e-02 ± 1.9e-03	1.00 ± 0.34	0.42 ± 0.10	? Galaxy J060740-665136 (MHH96), SEP
561	05 34 41.6	−67 38 31	45.1	6.18e-02 ± 1.2e-02	1.00 ± 0.15	−0.04 ± 0.15	AGN RX J05348-6739, z=0.0720 (CSM97)
876	05 32 01.3	−69 19 50	9.6	1.33e-02 ± 1.3e-03	1.00 ± 0.21	0.02 ± 0.09	AGN RXJ0532.0-6920 z=0.149 (SCF94)
1040	05 09 13.4	−69 54 12	14.3	4.32e-02 ± 4.5e-03	1.00 ± 0.27	0.28 ± 0.10	AGN Sy1, z=0.175 (WHHW91)
1094	05 24 01.6	−70 11 05	1.5	1.14e-01 ± 4.0e-03	0.91 ± 0.02	0.27 ± 0.04	AGN RXJ0524.0-7011 z=0.151 (SCF94)
1166	06 01 10.9	−70 36 14	6.0	8.73e-03 ± 1.4e-03	1.00 ± 0.65	0.34 ± 0.15	AGN (WBB87)
1231	06 02 56.3	−71 02 46	42.8	7.86e-03 ± 2.1e-03	1.00 ± 1.48	1.00 ± 2.33	? Galaxy (SEL95)
1243	05 50 31.5	−71 10 16	22.0	2.86e-03 ± 6.2e-04	1.00 ± 0.75	1.00 ± 1.61	AGN RX J0550.5-7109, z=0.4429 (CGC97)
1279	05 31 30.6	−71 28 49	66.4	1.44e-02 ± 1.7e-02	1.00 ± 0.38	1.00 ± 1.55	AGN RXJ0531.5-7130 z=0.2214 (SCF94)
1367	05 16 37.9	−72 37 01	99.1	6.53e-03 ± 8.5e-03	1.00 ± 1.75	1.00 ± 1.81	? AGN?, flat spectrum radio source (WBA91)

Table 9. Identification with foreground stars

1	2	3	4	5	6	7	8	9	10
No	RA (J2000.0)	Dec (J2000.0)	r_{90} [″]	Count Rate [cts s^{-1}]	HR1	HR2	dist [″]	$\log(f_x/f_{opt})$	Remarks
42	05 31 28.4	−64 05 49	15.8	9.73e-03 ± 2.7e-03	−0.17 ± 0.27		7.3	−3.5	foreground Star G3/G5, HD 37107 ()
61	05 43 33.5	−64 23 02	24.6	6.53e-02 ± 8.8e-03	−0.00 ± 0.13	0.05 ± 0.19	0.0		fg Star? (HP99)
78	05 36 21.7	−64 49 41	6.0	3.68e-02 ± 5.3e-03	0.53 ± 0.13	−0.06 ± 0.17	0.0	−1.8	fg Star? (HP99)
89	05 33 17.0	−65 01 12	40.2	1.98e-02 ± 5.6e-03	−1.00 ± 0.81		30.9	−1.2	foreground Star G1V, HD 37351 (O94)
96	05 23 50.3	−65 10 18	29.2	2.86e-02 ± 4.9e-03	1.00 ± 0.37	0.37 ± 0.15	30.1	−3.2	foreground Star F7V, HD 36023 ()
122	05 28 44.4	−65 26 59	0.6	8.07 ± 7.7e-02	−0.00 ± 0.01	0.07 ± 0.01	3.9	−2.0	foreground Star K0 (GGO93), AB Dor, HD 36705, (HP99)
157	05 44 47.2	−65 44 01	10.5	6.57e-03 ± 1.4e-03	−0.20 ± 0.22	−1.00 ± 0.63	8.2	−6.1	foreground Star A7V, HD 39014, IR excess (JJA91)
212	05 54 59.0	−65 57 38	42.5	5.87e-02 ± 3.7e-03	0.16 ± 0.06	0.12 ± 0.08	9.3	−3.6	fg Star F8IV/V, HD 40625, SEP
239	05 20 14.1	−66 04 27	8.5	1.42e-01 ± 4.9e-03	−0.14 ± 0.03	0.06 ± 0.05	8.3	−2.2	foreground Star G8V, (CCH84)
268	05 35 19.5	−66 12 51	31.3	3.35e-02 ± 4.9e-03	−0.24 ± 0.13	−1.00 ± 1.65	56.6	−1.4	? fg Star dM4e (CCH84)
272	06 00 15.2	−66 13 42	26.5	5.51e-03 ± 1.1e-03	−1.00 ± 2.90	1.00 ± 1.84	20.7	−1.8	fg Star F3V, HD 41466, SEP
273	05 19 57.5	−66 13 56	15.8	8.35e-02 ± 4.5e-03	0.05 ± 0.05	0.14 ± 0.07	6.1	−2.8	foreground Star G5, HD 269339 (GOG97)
279	04 58 14.3	−66 15 25	19.5	1.78e-03 ± 5.4e-04	1.00 ± 0.84		18.1	−4.7	foreground Star G6IV, HD 32427 ()
304	05 02 09.1	−66 20 38	4.1	2.74e-02 ± 2.0e-03	0.68 ± 0.06	0.08 ± 0.08	6.5	−2.4	foreground Star K0III, RXJ0502.2-6621 (SCF94)
310	05 02 56.6	−66 21 28	33.0	2.64e-03 ± 3.1e-03	1.00 ± 1.06		49.9	−4.2	? fg Star K2, HD 268879 (FD73)
336	05 26 05.6	−66 26 50	11.7	4.88e-03 ± 9.4e-04	−0.17 ± 0.19	−1.00 ± 1.27	10.9	−4.4	foreground Star F5V, HD 36356 (GGO93)
386	05 05 50.6	−66 35 08	61.8	8.82e-03 ± 1.3e-02			57.3		? fg Star A7, HD 268956 (GOG97)
439	05 37 10.1	−66 53 07	8.7	5.21e-02 ± 8.9e-03	0.14 ± 0.17	0.19 ± 0.22	0.0	−1.8	fg Star? (HP99)
477	05 35 38.3	−67 05 13	7.9	5.28e-02 ± 7.9e-03	−0.02 ± 0.15	0.19 ± 0.21	0.0		fg Star? (HP99)
478	05 30 49.4	−67 05 53	11.4	4.77e-02 ± 8.9e-03	−0.25 ± 0.18	0.34 ± 0.28	3.9		foreground Star dMe (SCF94, HP99)
487	05 08 55.3	−67 09 58	47.8	7.42e-03 ± 1.9e-03	1.00 ± 4.27		21.5	−2.9	foreground Star F5V, HD 33986 (GOG97)
509	05 15 59.1	−67 16 28	5.1	2.17e-02 ± 1.9e-03	−0.11 ± 0.09	0.26 ± 0.12	25.2		fg Star? (HP99)
586	05 02 44.2	−67 50 42	15.3	1.11e-02 ± 2.2e-03	1.00 ± 0.75	0.01 ± 0.22	14.8	−4.3	foreground Star G8/K0III, HD 33117 (ABM72)
595	05 25 02.8	−67 53 27	8.4	1.81e-02 ± 1.8e-03	0.38 ± 0.10	0.08 ± 0.12	0.0		foreground Star K2IV, RS CVn? (CSM97)
620	04 51 25.3	−68 03 36	65.8	9.85e-03 ± 2.1e-03			42.4	−4.9	? fg Star, HD 31532 (GGO93)
623	04 54 21.4	−68 04 27	46.0	7.52e-03 ± 1.5e-03	1.00 ± 0.73		18.4	−1.6	foreground Star ARDB 619, (ABM72)
636	05 16 06.6	−68 15 50	27.2	1.10e-01 ± 7.2e-03	−0.03 ± 0.06	−0.09 ± 0.09	13.2	−2.3	fg Star G1V (SCF94)
678	04 46 35.4	−68 32 30	60.9	2.25e-02 ± 3.2e-03	−0.35 ± 0.14		18.5	−4.4	foreground Star F7V, HD 30969 (GOG97)
693	05 27 00.0	−68 37 22	7.8	1.13e-02 ± 1.1e-03	−0.46 ± 0.09	−0.47 ± 0.16	0.9	−5.2	foreground Star F0IV-V, HD 36584 (GOG97)
729	04 56 35.3	−68 49 11	12.2	3.72e-03 ± 7.1e-04	1.00 ± 3.58	1.00 ± 1.95	30.9	−4.0	? fg Star HD 268799 (GGO93)
742	04 58 44.5	−68 50 58	6.5	1.23e-01 ± 6.0e-03	−0.04 ± 0.05	0.09 ± 0.07	21.7	−1.7	foreground Star dMe, HD 268840 (CSM97)
749	05 29 27.3	−68 52 03	2.4	1.44e-01 ± 3.5e-03	0.06 ± 0.02	0.04 ± 0.03	3.3	−2.7	foreground Star G2IV, HD 269620 (CSM97)
752	05 38 34.9	−68 53 03	1.2	2.98e-01 ± 4.8e-03	−0.04 ± 0.02	0.05 ± 0.02	23.1	−2.0	foreground Star G2V, RS CVn? (CSM97)
816	04 58 28.0	−69 08 39	26.1	1.22e-02 ± 1.7e-03	1.00 ± 0.51	0.29 ± 0.13	0.0	−3.0	foreground Star F7V (CSM97)
902	05 38 16.4	−69 23 30	1.4	1.72e-01 ± 4.6e-03	0.02 ± 0.03	−0.00 ± 0.04	4.8	−1.7	foreground Star dMe (CSM97)
935	05 16 45.5	−69 29 41	28.4	1.11e-01 ± 2.6e-02	0.15 ± 0.24	−1.00 ± 0.90	0.0	−2.3	fg Star? (HP99)
943	05 13 41.4	−69 31 50	17.5	2.42e-02 ± 4.5e-03			35.5	−2.9	foreground Star K1V (CSM97)
964	05 25 39.1	−69 35 42	3.5	3.29e-02 ± 2.6e-03	0.30 ± 0.08	−0.01 ± 0.10	4.1	−3.5	fg Star F7V, HD 36436 (CSM97)
1007	05 22 14.4	−69 46 02	25.2	5.87e-03 ± 8.8e-03	−1.00 ± 0.63		18.0	−2.3	foreground Star (GGO93), HD 269442
1008	05 30 10.5	−69 46 37	40.9	7.38e-03 ± 2.2e-03	1.00 ± 0.56	−1.00 ± 1.58	42.3	−4.2	? fg Star F2V (GGO93), HD 37121
1014	05 49 30.9	−69 47 23	12.6	9.33e-03 ± 2.4e-03	−1.00 ± 0.89		12.1	−4.1	foreground Star F2V (GGO93), HD 39904
1036	05 51 00.5	−69 53 26	60.9	5.99e-02 ± 8.9e-03	−0.11 ± 0.16	−1.00 ± 3.23	6.0	−3.8	foreground Star F5V:, HD 40156 (CSM97)
1093	05 25 57.6	−70 11 03	3.7	4.14e-02 ± 2.7e-03	0.68 ± 0.06	0.23 ± 0.07	0.0	−2.5	foreground Star K2IV-Vp, RS CVn (SCF94 HP99)
1147	05 13 00.8	−70 27 42	28.7	1.14e-01 ± 1.3e-02	−0.24 ± 0.11	−0.20 ± 0.18	8.6	−1.4	foreground Star dM4e, V12567 (CCH84)
1215	05 34 40.3	−70 56 18	6.9	2.12e-02 ± 1.7e-03	−0.36 ± 0.07	−0.07 ± 0.14	10.4	−3.7	foreground Star K1V, HD 37798 (GOG97)
1217	05 55 00.5	−70 57 20	56.0	6.32e-03 ± 9.0e-03		1.00 ± 0.55	41.8	−3.6	? fg Star K1/K2, HD 40871 ()
1220	05 47 34.2	−70 59 24	11.1	2.34e-03 ± 8.8e-04	−1.00 ± 0.85		4.1	−4.7	foreground Star F5V, HD 39675 (GOG97)
1242	05 23 58.5	−71 09 56	35.9	2.77e-01 ± 3.4e-02	−0.17 ± 0.12	0.24 ± 0.19	36.2	−1.1	foreground Star dM5e (CCH84)
1272	06 04 30.6	−71 25 29	22.0	1.76e-02 ± 2.7e-03	1.00 ± 0.50	0.46 ± 0.12	22.4	−1.8	foreground Star, Dwarf Nova V* AD Men (DWS97)
1280	05 19 55.0	−71 29 22	24.3	1.34e-02 ± 1.8e-03	0.30 ± 0.13	0.35 ± 0.10	0.0	−3.7	foreground Star K2III, RXJ0519.9-7129 (SCF94)
1284	05 17 27.8	−71 31 46	19.0	1.90e-02 ± 2.0e-03	1.00 ± 0.79	−0.09 ± 0.10	13.3	−4.4	foreground Star K2III (GGO93), HD 35324
1322	05 17 48.3	−71 55 27	12.2	2.70e-03 ± 6.5e-04	1.00 ± 1.43	−1.00 ± 0.67	5.5	−4.3	foreground Star A8V (GGO93), HD 35434
1327	05 18 57.4	−71 58 20	5.2	7.00e-03 ± 9.1e-04	1.00 ± 0.39	0.58 ± 0.12	24.1	−1.7	? fg Star (GGO93), HD 35569
1334	06 18 23.2	−72 02 43	9.1	7.63e-01 ± 1.8e-02	−0.08 ± 0.02	0.01 ± 0.03	23.3	−1.6	foreground Star K3:V:, HD 45081, 2RE J0618-720 (PMA95)
1352	05 16 05.1	−72 14 24	35.8	5.35e-03 ± 1.6e-03	−1.00 ± 0.91		44.9	−3.3	? fg Star M2, LHS 1749
1355	05 40 57.7	−72 16 21	72.9	1.97e-02 ± 3.7e-03	−0.01 ± 0.17	1.00 ± 3.45	10.0	−3.9	foreground Star F6V, HD 38728 ()
1358	05 22 45.7	−72 20 14	13.8	2.40e-02 ± 1.9e-03	0.50 ± 0.08	0.32 ± 0.09	5.4	−4.3	foreground Star A6III, HD 36145 (T80)

Table 10. Classified PSPC sources

1	2	3	4	5	6	7	8	9	10	11
No	ML_{exi}	RA	Dec	r_{90}	Count Rate	HR1	HR2	Extent	ML_{ext}	Remarks
		(J2000.0)		[″]	[cts s^{-1}]			[″]		
1	88.2	05 40 20.5	−62 41 15	44.9	1.65e-01 ± 1.8e-02	0.35 ± 0.11	0.12 ± 0.13	75.7	5.1	[AGN]
37	98.0	05 52 21.4	−64 02 16	43.1	1.75e-01 ± 1.9e-02	0.57 ± 0.11	0.17 ± 0.12	80.5	7.4	[AGN] PMNJ0552-6401
46	165.1	05 46 05.9	−64 07 11	7.0	4.91e-02 ± 6.1e-03	−0.08 ± 0.12	0.26 ± 0.18	6.5	0.5	[fg Star]
49	85.5	05 44 59.7	−64 11 33	36.2	3.29e-02 ± 3.5e-03	0.19 ± 0.12	0.46 ± 0.06	48.4	1.9	[fg Star]
58	20.6	05 28 26.7	−64 17 37	51.0	2.94e-02 ± 6.5e-03	−0.14 ± 0.21	1.00 ± 1.33	0.0	0.0	[fg Star]
83	32.5	05 38 31.5	−64 56 24	10.8	1.17e-02 ± 3.0e-03	−0.27 ± 0.25	1.00 ± 3.18	0.0	0.0	[fg Star]
88	35.5	05 29 41.9	−65 00 33	29.3	2.01e-02 ± 3.7e-03	0.17 ± 0.19	0.36 ± 0.21	18.4	0.3	[fg Star] GSC 8887.0754
93	201.9	05 37 22.8	−65 04 07	11.5	8.61e-02 ± 8.4e-03	1.00 ± 0.18	0.57 ± 0.09	29.0	78.4	[SNR] GSC 8887.0518, GSC-ext, const
101	172.8	05 41 37.5	−65 11 33	32.8	8.61e-02 ± 7.5e-03	1.00 ± 0.20	0.32 ± 0.08	88.8	33.9	[hard] Galaxy? (DSS)
107	173.6	05 21 48.5	−65 18 58	6.0	9.53e-03 ± 1.2e-03	1.00 ± 0.26	0.10 ± 0.12	5.1	0.3	[stellar] GSC 8886.0790
110	29.3	05 36 06.0	−65 22 01	97.6	1.58e-02 ± 1.6e-02	1.00 ± 0.15	0.22 ± 0.06	143.8	11.1	[hard]
113	100.5	05 19 09.7	−65 25 11	7.3	6.99e-03 ± 1.1e-03	1.00 ± 0.22	0.49 ± 0.14	5.1	0.2	[hard]
146	114.8	05 35 08.3	−65 38 29	8.2	3.15e-02 ± 4.4e-03	0.51 ± 0.13	0.25 ± 0.16	3.0	0.0	[fg Star] GSC 8891.0777
147	46.6	05 28 50.2	−65 39 38	15.2	1.58e-02 ± 2.9e-03	1.00 ± 0.15	0.27 ± 0.18	20.6	11.7	[hard]
153	10.3	05 28 34.9	−65 42 34	29.7	1.53e-03 ± 1.9e-03	0.65 ± 0.06	−0.50 ± 0.05	16.1	0.5	[fg Star] GSC 8891.0979
183	357.1	05 30 10.6	−65 51 27	2.8	6.00e-03 ± 4.5e-04	1.00 ± 0.21	0.62 ± 0.07	1.6	0.0	[hard]
190	20.4	05 32 28.7	−65 53 50	19.8	5.91e-03 ± 5.9e-03	1.00 ± 0.09	0.16 ± 0.11	37.1	36.8	[hard]
228	11.9	05 24 51.5	−66 02 20	23.6	2.96e-03 ± 8.6e-04	1.00 ± 0.04	−0.04 ± 0.03	8.2	0.1	[hard]
230	77.4	05 34 24.5	−66 02 47	20.6	1.39e-02 ± 1.3e-03	1.00 ± 0.02	1.00 ± 0.08	44.2	18.7	[hard]
233	193.7	05 29 00.6	−66 03 04	5.1	6.18e-03 ± 5.3e-04	1.00 ± 0.22	0.07 ± 0.08	7.6	1.4	[hard]
255	115.8	05 55 02.8	−66 09 00	32.4	3.15e-02 ± 2.5e-03	0.07 ± 0.08	−0.18 ± 0.11	58.4	4.2	[fg Star] GSC 8904.0735, SEP
258	211.1	05 59 44.1	−66 09 16	10.3	1.86e-02 ± 1.3e-03	0.16 ± 0.07	−0.15 ± 0.09	17.6	2.2	[fg Star], SEP
276	44.7	05 35 51.2	−66 15 16	17.6	8.12e-03 ± 1.2e-03	−0.24 ± 0.05	0.01 ± 0.09	19.5	2.1	[fg Star]
283	16.3	05 00 19.2	−66 16 23	13.3	2.77e-03 ± 1.1e-03	−1.00 ± 1.15		0.0	0.0	[stellar] GSC 8889.0315
301	19.4	05 27 39.9	−66 20 01	11.5	1.88e-03 ± 5.8e-04	1.00 ± 0.42	1.00 ± 1.60	0.0	0.0	[stellar] GSC 8891.1771 or GSC 8891.1739
305	189.7	05 24 12.7	−66 20 50	7.0	1.17e-02 ± 1.2e-03	1.00 ± 0.14	0.67 ± 0.08	9.4	1.7	[hard]
311	406.2	06 07 53.4	−66 21 37	20.3	7.60e-02 ± 3.3e-03	0.16 ± 0.04	0.16 ± 0.05	54.3	9.6	[fg Star] GSC 8905.0616, SEP
330	55.8	05 22 19.3	−66 25 56	24.3	1.52e-02 ± 1.9e-03	−0.24 ± 0.13	1.00 ± 1.87	32.5	3.3	? [fg Star]
344	37.3	05 37 31.9	−66 28 27	40.9	1.38e-02 ± 2.0e-03	1.00 ± 0.20	−0.07 ± 0.13	61.2	11.6	[hard]
366	11.6	05 31 23.8	−66 32 18	16.3	1.49e-03 ± 5.0e-04	1.00 ± 1.38	1.00 ± 1.91	0.0	0.0	[stellar] GSC 8891.0704
372	79.3	04 52 20.8	−66 32 59	23.2	8.51e-03 ± 1.3e-03	1.00 ± 0.10	1.00 ± 0.90	33.4	3.4	[hard]
377	19.8	04 59 31.3	−66 33 36	12.9	2.87e-03 ± 7.0e-04	1.00 ± 1.90	1.00 ± 2.47	0.0	0.0	[stellar] GSC 8889.0423
418	42.0	05 57 46.0	−66 44 55	21.6	4.96e-03 ± 8.7e-04	1.00 ± 0.23	0.34 ± 0.15	28.7	5.2	[hard], SEP
424	76.0	06 03 13.6	−66 46 19	12.1	8.50e-03 ± 9.7e-04	−0.15 ± 0.11	0.06 ± 0.17	12.0	0.9	[fg Star], SEP
442	31.2	04 56 46.1	−66 53 22	15.2	4.84e-03 ± 9.1e-04			4.8	−0.0	[stellar] GSC 8889.0627
443	31.9	04 58 11.2	−66 53 24	26.7	5.20e-03 ± 3.9e-03	1.00 ± 0.17	0.23 ± 0.16	13.3	0.1	[hard]
482	152.5	04 52 50.0	−67 07 19	7.2	7.82e-03 ± 9.4e-04	1.00 ± 0.16	0.39 ± 0.11	9.3	1.8	[hard] RX J0452.8-6707 (no ID in SCL94)
490	18.9	04 57 37.1	−67 11 24	15.0	2.31e-03 ± 6.3e-04	1.00 ± 0.89	−0.18 ± 0.26	0.0	0.0	[stellar] GSC 8889.0342
494	78.7	05 29 47.2	−67 13 54	12.3	4.87e-02 ± 7.9e-03	0.50 ± 0.15	0.25 ± 0.19	11.3	1.0	[stellar] GSC 8891.3619
495	29.0	05 26 04.0	−67 14 00	12.4	1.06e-02 ± 2.3e-03	1.00 ± 1.44	−0.52 ± 0.21	5.2	0.1	[stellar] GSC 8891.3622
520	89.8	04 53 32.0	−67 20 32	11.9	1.05e-02 ± 1.2e-03	−0.10 ± 0.11	0.60 ± 0.13	20.3	6.7	[fg Star] RX J0453.5-6720 (no ID in SCL94)
529	58.4	05 04 49.5	−67 24 15	40.6	2.16e-02 ± 2.5e-03	1.00 ± 0.20	−0.29 ± 0.11	63.1	10.1	[SNR]
530	39.6	05 13 40.5	−67 24 21	12.4	5.39e-03 ± 9.9e-04	1.00 ± 0.21	0.15 ± 0.17	17.5	13.0	[hard]
545	53.5	05 12 23.1	−67 32 15	12.5	5.21e-03 ± 1.0e-03	1.00 ± 0.20	1.00 ± 0.95	6.2	0.1	[hard]
564	34.2	05 23 20.2	−67 41 37	20.8	1.30e-02 ± 1.9e-03	1.00 ± 0.23	−0.13 ± 0.14	34.8	20.5	[SNR] no HRI detection by (CSM97)
568	457.0	05 05 28.1	−67 43 16	3.4	4.44e-02 ± 3.6e-03	0.74 ± 0.06	0.18 ± 0.09	0.0	0.0	[fg Star] GSC 9161.1103
632	81.2	04 54 37.9	−68 11 19	21.7	1.47e-02 ± 1.7e-03	0.09 ± 0.10	−1.00 ± 1.62	33.7	5.0	[fg Star]

Table 10. continued

1	2	3	4	5	6	7	8	9	10	11
No	ML_{exi}	RA	Dec	r_{90}	Count Rate	HR1	HR2	Extent	ML_{ext}	Remarks
		(J2000.0)		[″]	[cts s^{-1}]			[″]		
653	85.1	04 36 10.3	−68 22 16	29.8	5.26e-02 ± 6.5e-03	1.00 ± 0.14	0.14 ± 0.12	64.2	34.1	[hard] Galaxy? (DSS)
673	27.9	04 56 26.4	−68 30 43	16.4	2.93e-03 ± 6.6e-04	1.00 ± 0.19	−0.45 ± 0.18	20.0	6.3	[SNR]
724	77.6	05 07 37.9	−68 47 49	7.1	7.74e-03 ± 1.2e-03	1.00 ± 0.16	−0.02 ± 0.16	4.8	0.2	[hard]
728	63.9	05 29 23.8	−68 49 08	10.9	7.17e-03 ± 9.3e-04	0.23 ± 0.14	0.02 ± 0.17	13.2	1.8	[fg Star]
747	46.8	05 46 48.3	−68 51 47	48.7	1.52e-02 ± 1.3e-02	1.00 ± 0.21	1.00 ± 0.60	12.6	−0.0	[hard] RX J0547.0-6852 (no ID in SCF94)
776	247.4	05 43 03.5	−68 59 15	26.9	2.44e-01 ± 8.4e-03	1.00 ± 0.06	−0.13 ± 0.03	34.9	2.3	[SNR]
796	263.1	04 58 24.9	−69 03 53	16.4	2.85e-02 ± 2.2e-03	1.00 ± 0.07	0.59 ± 0.06	47.1	28.0	[hard]
803	46.4	04 55 37.3	−69 05 32	25.8	1.12e-02 ± 1.8e-03	1.00 ± 0.19	0.14 ± 0.14	35.5	6.0	[hard]
830	126.2	05 06 37.1	−69 10 44	21.6	3.26e-02 ± 3.4e-03	1.00 ± 0.08	0.22 ± 0.09	46.5	13.4	[hard]
887	19.0	05 18 24.7	−69 21 26	27.0	1.60e-02 ± 3.8e-03	0.43 ± 0.12	−0.34 ± 0.14	17.7	0.6	[fg Star] GSC 9162.0126
913	229.4	04 56 24.2	−69 26 02	42.8	1.39e-01 ± 6.5e-03	1.00 ± 0.10	−0.16 ± 0.04	216.7	293.2	[SNR] LMC Star cluster LH 8 (WH91), diffuse, far offaxis
931	39.1	05 22 46.9	−69 28 34	12.0	8.87e-03 ± 1.6e-03	1.00 ± 0.19	0.32 ± 0.16	6.6	0.1	[hard]
954	12.6	05 23 14.0	−69 33 38	15.5	7.13e-03 ± 2.5e-03	1.00 ± 0.50		0.0	0.0	[stellar] GSC 9166.0446
1024	66.1	05 52 29.4	−69 49 12	33.9	7.30e-02 ± 1.3e-02	1.00 ± 0.14	0.46 ± 0.15	23.4	0.3	[hard]
1057	13.4	05 49 46.9	−70 00 09	99.6	4.78e-02 ± 9.4e-03	0.43 ± 0.10	−1.00 ± 0.17	115.3	13.1	[SSS]
1063	109.2	05 39 36.2	−70 01 44	10.2	2.36e-02 ± 2.6e-03	1.00 ± 0.17	−0.17 ± 0.10	18.2	7.7	[SNR], const
1109	76.6	05 23 12.8	−70 15 21	11.2	1.07e-02 ± 1.6e-03	1.00 ± 0.16	0.15 ± 0.14	16.0	3.8	[hard]
1113	14.2	05 24 59.6	−70 16 24	31.4	3.41e-03 ± 1.1e-03	0.91 ± 0.02	0.27 ± 0.04	28.3	3.2	[hard]
1124	158.5	05 34 08.2	−70 18 58	5.0	1.31e-02 ± 1.6e-03	1.00 ± 0.19	0.46 ± 0.11	0.0	0.0	[hard]
1140	10.8	05 35 34.5	−70 26 05	49.6	6.87e-03 ± 3.4e-03		−1.00 ± 0.27	37.3	2.4	[SSS]
1146	129.0	05 43 40.7	−70 27 11	49.4	1.12e-01 ± 6.8e-03	1.00 ± 0.07	0.27 ± 0.07	161.6	189.8	[hard] diffuse, offaxis
1155	90.7	05 35 30.6	−70 30 09	10.9	1.18e-02 ± 1.3e-03	−0.07 ± 0.10	−0.66 ± 0.11	16.1	2.6	[fg Star] GSC 9166.0106
1171	14.9	05 31 59.4	−70 38 19	21.8	3.50e-03 ± 5.0e-03	1.00 ± 0.73	−1.00 ± 0.24	0.0	0.0	[SSS]
1179	142.8	05 47 05.5	−70 40 37	18.1	1.27e-02 ± 1.3e-03	1.00 ± 0.09	0.30 ± 0.11	28.5	2.9	[hard]
1181	248.5	05 36 00.7	−70 41 28	3.7	1.03e-02 ± 1.1e-03	1.00 ± 0.14	0.39 ± 0.10	0.0	0.0	[hard] RX J0536.0-7041 (no ID in CSM97)
1184	236.8	06 06 02.1	−70 42 07	20.8	5.45e-02 ± 4.5e-03	1.00 ± 0.15	0.52 ± 0.07	56.8	22.5	[AGN] PMNJ0606-7041, Galaxy? (DSS)
1189	41.7	06 03 22.2	−70 43 58	18.2	6.17e-03 ± 1.2e-03	1.00 ± 0.20	0.12 ± 0.20	17.0	1.0	[hard] AGN? (position)
1194	29.1	05 52 07.0	−70 46 55	51.2	1.74e-02 ± 2.3e-03	−0.31 ± 0.11	−0.12 ± 0.16	52.9	3.1	[fg Star]
1228	185.4	05 30 21.9	−71 01 50	24.1	7.02e-02 ± 4.9e-03	1.00 ± 0.07	−0.14 ± 0.06	98.5	105.4	[SNR] diffuse, offaxis
1229	14.4	05 43 32.0	−71 02 06	27.9	7.65e-04 ± 1.4e-03	1.00 ± 0.13	1.00 ± 0.15	13.0	0.3	[hard]
1234	33.4	05 27 57.2	−71 04 30	59.5	1.44e-02 ± 3.0e-03	1.00 ± 0.71	−0.31 ± 0.16	39.4	0.2	[SNR]
1247	312.0	05 48 28.7	−71 12 41	3.2	8.27e-03 ± 7.1e-04	1.00 ± 0.09	0.27 ± 0.08	3.0	0.2	[hard]
1268	50.2	05 22 57.6	−71 24 46	51.5	1.69e-02 ± 2.8e-03	1.00 ± 0.12	0.36 ± 0.11	78.1	7.0	[hard]
1277	402.4	06 07 08.4	−71 27 45	4.9	3.72e-02 ± 2.7e-03	−0.01 ± 0.08	−0.07 ± 0.10	8.4	2.3	[fg Star] GSC 9172.1143
1293	106.4	06 08 43.6	−71 36 51	6.2	1.21e-02 ± 1.6e-03	0.27 ± 0.14	−0.21 ± 0.16	0.0	0.0	[fg Star] GSC 9172.1117, GSC-ext
1294	21.2	06 11 13.3	−71 37 27	13.1	4.28e-03 ± 1.1e-03	1.00 ± 3.09	−1.00 ± 1.90	0.0	0.0	[stellar] GSC 9172.1176
1305	51.7	05 17 49.7	−71 44 04	12.2	8.54e-03 ± 1.3e-03	1.00 ± 1.34	0.45 ± 0.15	2.5	−0.0	[stellar] GSC 9170.2189
1312	623.1	05 49 47.9	−71 49 33	2.9	4.12e-02 ± 2.5e-03	−0.02 ± 0.06	−0.16 ± 0.08	0.0	0.0	[fg Star] GSC 9171.0288, GSC-ext
1320	40.6	05 29 36.9	−71 53 53	51.0	2.26e-02 ± 3.0e-03	−0.23 ± 0.11	−1.00 ± 2.52	42.3	0.8	[fg Star]
1335	32.6	05 16 35.7	−72 03 09	17.5	6.58e-03 ± 1.2e-03	−0.33 ± 0.17		12.5	0.6	[fg Star] GSC 9170.0952
1337	52.7	05 18 11.0	−72 03 52	8.9	5.40e-03 ± 8.4e-04	−0.14 ± 0.15	−0.30 ± 0.20	0.0	0.0	[fg Star]
1345	135.8	05 16 25.6	−72 06 54	9.8	1.62e-02 ± 1.6e-03	1.00 ± 0.71	−0.07 ± 0.11	13.8	2.6	[stellar] GSC 9170.0047
1346	79.7	05 48 00.5	−72 07 35	13.1	9.07e-03 ± 1.4e-03	1.00 ± 0.23	0.15 ± 0.14	17.3	4.0	[hard]
1349	12.0	05 20 11.3	−72 12 59	16.9	2.17e-03 ± 6.7e-04	1.00 ± 0.99	−1.00 ± 1.67	0.0	0.0	[stellar] GSC 9170.1015
1350	192.2	06 11 31.5	−72 13 39	26.8	9.66e-02 ± 7.0e-03	−0.07 ± 0.07	−0.13 ± 0.10	45.5	2.2	[fg Star] GSC 9172.1315